

MASARYKOVA UNIVERZITA
PŘÍRODOVĚDECKÁ FAKULTA
ÚSTAV TEORETICKÉ FYZIKY A ASTROFYZIKY

Diplomová práce

BRNO 2016

ZDENĚK PRUDIL



MASARYKOVA UNIVERZITA
PŘÍRODOVĚDECKÁ FAKULTA
ÚSTAV TEORETICKÉ FYZIKY A ASTROFYZIKY



Blažkův jev u hvězd typu RR Lyrae v Galaktické výduti

Diplomová práce

Zdeněk Prudil

Vedoucí práce: Mgr. Marek Skarka, Ph.D. Brno 2016

Bibliografický záznam

Autor: Bc. Zdeněk Prudil
Přírodovědecká fakulta, Masarykova univerzita
Ústav teoretické fyziky a astrofyziky

Název práce: Blažkův jev u hvězd typu RR Lyrae v Galaktické výduťi

Studijní program: Fyzika

Studijní obor: Teoretická fyzika a astrofyzika

Vedoucí práce: Mgr. Marek Skarka, Ph.D.

Akademický rok: 2015/2016

Počet stran: XI + 55

Klíčová slova: Blažkův jev; hvězdy typu RR Lyrae; Galaktická výduť; OGLE-IV; Fourierovy koeficienty; Oosterhoffova dichotomie

Bibliographic Entry

Author: Bc. Zdeněk Prudil
Faculty of Science, Masaryk University
Department of Theoretical Physics and
Astrophysics

Title of Thesis: Blazhko effect in Galactic bulge RR Lyrae stars

Degree Programme: Physics

Field of Study: Theoretical physics and astrophysics

Supervisor: Mgr. Marek Skarka, Ph.D.

Academic Year: 2015/2016

Number of Pages: XI + 55

Keywords: Blazhko effect; RR Lyrae stars; Galactic bulge; OGLE-IV; Fourier coefficients; Oosterhoff dichotomy

Abstrakt

Předložená diplomová práce se zabývá hledáním modulace světelných křivek, známé jako Blažkův jev, u hvězd typu RR Lyrae pulzujících v základním módu pulzací, které se nacházejí v Galaktické výduti a byly pozorovány přehlídkou OGLE-IV. Ve frekvenčním spektru se Blažkův jev nejvýrazněji projevuje ve formě ekvidistantních píků v blízkosti hlavní pulzační frekvence a jejích násobků. Proto je tato práce založena na hledání těchto příznaků. Pro zrychlení analýzy byly automaticky odstraněny složky hlavní pulzační frekvence a výsledná rezidua byla následně analyzována pomocí programu PERIOD04.

Z celkového souboru 8 283 hvězd 38 % hvězd vykazovalo Blažkův jev, 58 % nevykazovalo žádné známky modulace a zbylá 4 % hvězd byla označena jako kandidáti na Blažkovu modulaci. Nalezený poměr modulovaných hvězd vůči nemodulovaným je vyšší než bylo udáváno v předchozích studiích. Periody Blažkovy modulace se pohybují v rozsahu od 4.85 dne až po 2 198 dní, jejichž medián je 60.45 dne. Spodní limit modulačních period rovněž zastupuje nekratší známou Blažkovu periodu. Z analyzovaných dat není patrná žádná souvislost mezi pulzační a modulační periodou. Rovněž bylo zjištěno, že hvězdy s Blažkovým jevem se vyznačují nepatrně kratšími periodami (přibližně o 0.03 dne) a nižšími amplitudami (přibližně o 0.028(45) mag) v porovnání s hvězdami bez modulace. Průměrná pulzační perioda pro nemodulované hvězdy je rovna 0.56(9) dne, zatímco pro modulované hvězdy je průměr roven 0.53(6) dne, tudíž je rozdíl mezi oběma průměry v rámci chyby.

Dále byly nalezeny výrazné rozdíly ve Fourierových koeficientech R_{21} , R_{31} , φ_{21} a φ_{31} . Modulované hvězdy se kloní k nižším hodnotám těchto parametrů. Značný rozdíl mezi Blažkovými a nemodulovanými hvězdami je vidět hlavně v závislostech R_{31} na φ_{31} a R_{31} na φ_{21} . Díky tomu bylo možné odvodit vztahy sloužící k identifikaci modulovaných hvězd pomocí Fourierových koeficientů φ_{21} , φ_{31} a R_{31} . Rozdíly v metalicitě a prostorovém rozložení mezi modulovanými a nemodulovanými hvězdami nebyly nalezeny.

Vůbec poprvé bylo možné studovat rozdělení modulovaných a nemodulovaných hvězd mezi Oosterhoffovými skupinami v Galaktické výduti. Bylo zjištěno, že ve skupině OoI 46 % hvězd vykazuje Blažkův jev, zatímco ve OoII pouze 19 % hvězd projevuje Blažkovu modulaci. V průběhu analýzy byly objeveny doposud neznámé hvězdy typu RR Lyrae, které pulzují ve dvou módech zároveň s poměrem period přibližně 0.7.

Abstract

This thesis is focused on a search for light-curve modulation (known as the Blazhko effect) in fundamental-mode RR Lyrae stars in the Galactic bulge observed by OGLE-IV survey. Because the Blazhko effect produces additional equidistant peaks in the vicinity of the basic pulsation frequency components in frequency spectra, we searched for such patterns. For acceleration of the analysis, the main pulsation frequency components were prewhitened, and the residuals were analysed using PERIOD04 software.

We found that in a total sample of 8 283 RRab stars 38 % of the stars exhibit the Blazhko effect, 58 % show no sign of modulation, and remaining 4 % of the stars were marked as Blazhko candidates. The fraction of identified Blazhko stars is higher, than in previous studies. The modulation periods span from 4.85 to 2 198 days with the median value at 60.45 days. The bottom limit of the modulation-period distribution represents the shortest modulation period ever detected. We did not find any apparent relation between modulation and pulsation periods. It was found that the Blazhko stars are characterized by slightly shorter pulsation periods of a factor of 0.03 days and amplitudes lower of 0.028(45) mag than stars with stable light curve. The average pulsation period for modulated stars is 0.53(6) days, while for unmodulated counterparts is the average 0.56(9) days. Therefore the difference in pulsation periods is within error.

The substantial differences in Fourier coefficients R_{21} , R_{31} , φ_{21} and φ_{31} , were detected. Modulated stars seem to favour lower values of these parameters. Large difference between Blazhko stars and stable stars is seen in R_{31} on φ_{31} and R_{31} on φ_{21} dependences. Equations that can be used for identification of modulated stars based on Fourier parameters φ_{21} , φ_{31} and R_{31} were derived. We did not find any differences in metallicity or spatial distribution between modulated and unmodulated RR Lyraes.

For the first time, we could study the ration between modulated and unmodulated stars in the Oosterhoff groups in the Galactic bulge. We found, that in the OoI 46 % of stars show the Blazhko modulation, while in the OoII only 19 % stars exhibit the Blazhko effect. During our analysis we identified a completely new group of double-mode RR Lyrae pulsators with period ratio around 0.7 during our analysis.



Masarykova univerzita



Přírodovědecká fakulta

ZADÁNÍ DIPLOMOVÉ PRÁCE

Student : Bc. Zdeněk Prudil, učo 394480

Studijní program : Fyzika

Studijní obor : Teoretická fyzika a astrofyzika

Ředitel Ústavu teoretické fyziky a astrofyziky PřF MU Vám ve smyslu Studijního a zkušebního řádu MU určuje diplomovou práci s tématem:

Blazhko effect in Galactic bulge RR Lyrae stars

Blazhko effect in Galactic bulge RR Lyrae stars

Zásady pro vypracování: Currently it is largely accepted that almost a half of RR Lyrae type stars exhibits modulation of the light curve. This phenomenon, known as the Blazhko effect, represents a still unexplained problem. It is not clear why some stars show modulation and others not, what is the physical difference between Blazhko and regular RR Lyrae stars, and what actually stands behind the modulation. In addition, astronomers still do not know what is the relation between modulation and pulsation periods, and what is the true percentage of modulated stars among RR Lyrae pulsators. The later two problems are considered to be investigated in this work. Data for several thousands of fundamental mode RR Lyrae stars located in the Galactic bulge observed by the OGLE IV survey represent a perfect sample for this kind of study. Thus the main objective is to discover the Blazhko effect and to describe its properties in a large number of stars. Since a huge amount of data will be analysed, it is assumed that new semiautomatic procedures and methods will be developed to properly identify the modulation. Results will be interpreted in a statistical way and compared with current knowledge of the Blazhko effect.

Literatura:


- AERTS, Conny, Jorgen CHRISTENSEN-DALSGAARD a Donald W. KURTZ. *Asteroseismology*. Netherlands: Springer Science+Business Media, 2010. ISBN 978-1-4020-5178-4.
Změněno: 16. 12. 2014 12:45, Mgr. Marek Skarka, Ph.D.
- MIKULÁŠEK, Zdeněk a Miloslav ZEJDA. *Proměnné hvězdy*. ÚTFA PřF MU. Brno, 2009.
Změněno: 16. 12. 2014 12:45, Mgr. Marek Skarka, Ph.D.
- SMITH, Horace A. *RR Lyrae stars*. Cambridge: Cambridge university press, 1995. 168 s. ISBN 978-0-521-54817-5.
Změněno: 16. 12. 2014 12:45, Mgr. Marek Skarka, Ph.D.

Jazyk závěrečné práce : český, anglický nebo slovenský
Vedoucí diplomové práce : Mgr. Marek Skarka, Ph.D.
Konzultant : Mgr. Jiří Liška
Datum zadání diplomové práce : leden 2015
Datum odevzdání diplomové práce : dle harmonogramu ak. roku 2015/2016

V Brně leden 2015


Rikard von Unge
ředitel ÚTFA

Zadání diplomové práce převzal dne: 16/2 2014


Podpis studenta

Poděkování

Na tomto místě bych chtěl hlavně poděkovat svému vedoucímu Mgr. Marku Skarkovi, Ph.D. za cenné konzultace, věnovaný čas, klíčové korekce a vedení, bez kterého by tato práce jen těžko vznikla.

Díky patří rovněž Mgr. Jiřímu Liškovi, Ph.D. za opravy textu a rady, které pomohly pozvednout tuto práci. S díky nelze zapomenout na Reinholda, Aničku a tedy vlastně celý tým SERMON. Za korekci gramatiky rovněž děkuji paní Suchomelové-Polomské M.A.. Rád bych také poděkoval svým spolužákům a vyučujícím, díky kterým jsem tu prožil báječných pět let.

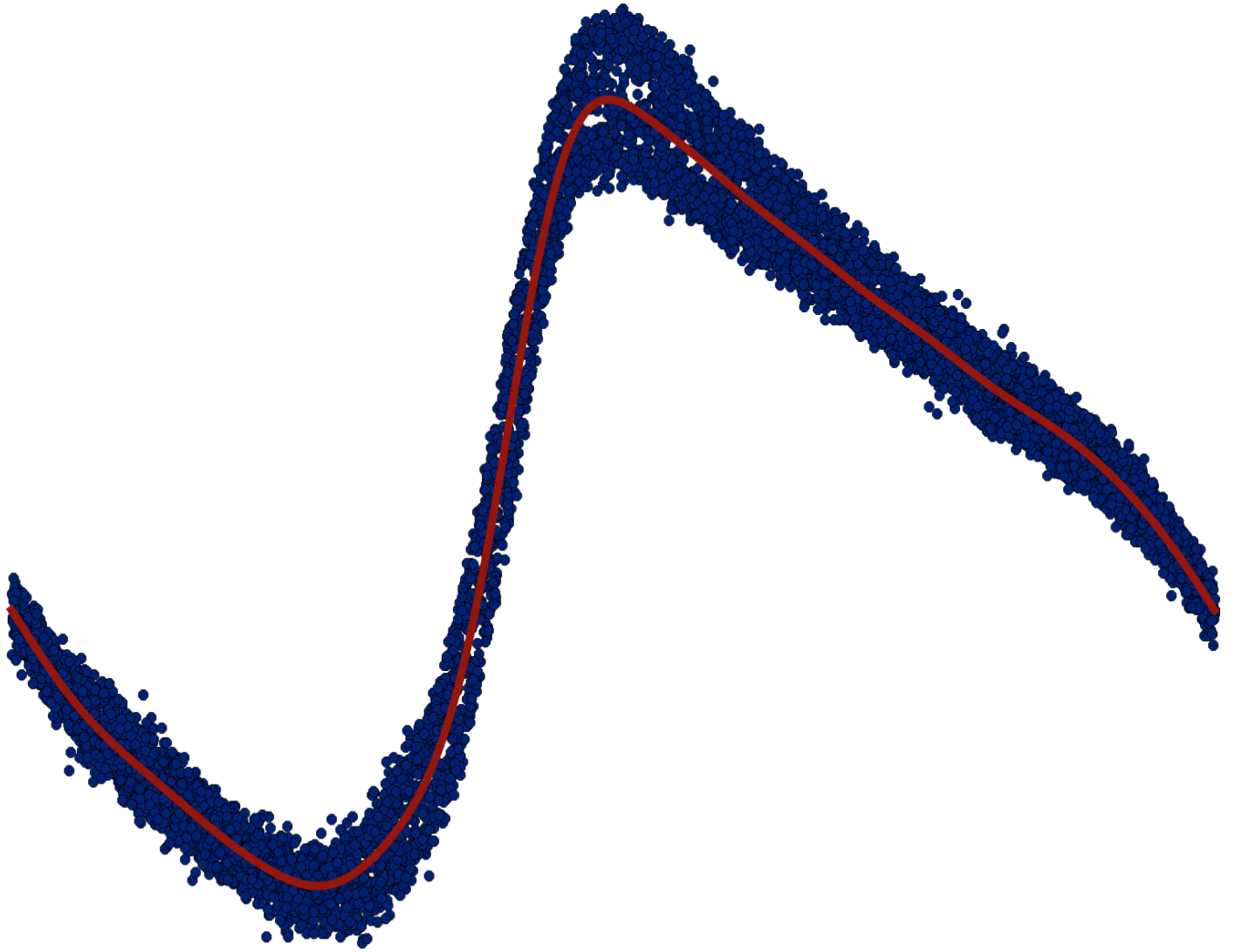
Děkuji také přítelkyni Vendy a rodičům za jejich podporu a trpělivost. Bez nich by nic z toho nebylo možné.

Prohlášení

Prohlašuji, že jsem svoji diplomovou práci vypracoval samostatně s využitím informačních zdrojů, které jsou v práci citovány.

Brno 11. května 2016

.....
Zdeněk Prudil



Contents

Chapter 1. A general overview of RR Lyrae stars	1
1.1 Types of RR Lyrae stars	2
1.2 The Oosterhoff dichotomy	4
1.3 The mechanism of pulsation	5
1.4 Multi-mode oscillation in RR Lyraes	7
Chapter 2. The least-squares method	9
2.1 Linear least-squares method	10
2.2 Non-linear least-squares method	11
2.2.1 Levenberg–Marquardt algorithm	12
2.2.2 Trigonometric polynomial	12
2.3 The Fourier coefficients	14
Chapter 3. The Blazhko effect	15
3.1 Frequency spectra of RR Lyrae stars	16
3.2 The occurrence of the Blazhko effect	19
3.3 The length of the Blazhko modulation	20
3.4 Differences between modulated and unmodulated stars	21
3.5 Physical models of the Blazhko effect and period doubling	22
Chapter 4. OGLE survey and data acquisition	23
4.1 OGLE-IV	24
4.2 Sample selection	25
4.3 Semi-automatic analysis	27
Chapter 5. Results	29
5.1 Fraction of Blazhko stars	29
5.2 Period distribution	31
5.3 Amplitude distribution	35
5.4 Fourier coefficients R_{21} and R_{31}	37
5.5 Fourier coefficients φ_{21} and φ_{31}	39
Chapter 6. By-product results	45
6.1 Oosterhoffs populations within the Galactic bulge	45

6.2 A new group of double-mode RR Lyrae pulsators	47
Chapter 7. Summary	50
Bibliography	52

Chapter 1

A general overview of RR Lyrae stars

RR LYRAE stars are radially pulsating variables, usually found in old stellar populations, thus, they are evolved horizontal branch stars, burning helium in their cores. They are located in the instability strip¹ in the Hertzsprung-Russell diagram (hereafter referred to as HRD), Fig. 1.1. They are one of the cornerstones of the study of stellar pulsation and evolution. RR Lyrae variables serve as excellent distance indicators which make them invaluable in investigating a galactic structure, dynamics, and mapping dense stellar regions (Pietrukowicz et al., 2015).

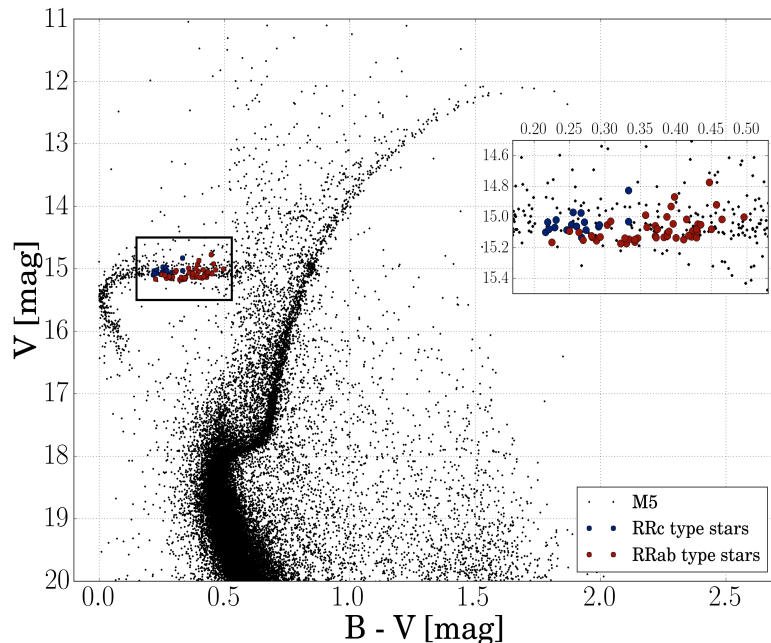


Figure 1.1: HRD for globular cluster M5 shown on data from [Viaux et al. \(2013\)](#) and data for RR Lyrae stars from [Szeidl et al. \(2011\)](#).

¹The instability strip is a narrow bar (width around 0.3 mag in $B - V$) stretching across the HRD.

The first detection and studies of RR Lyrae variables date back to the end of 19th century, to Edward Charles Pickering, Solomon Bailey and Harlow Shapley. They studied globular clusters and found short period variable stars with light curves similar to Cepheids. Later [Pickering \(1901\)](#) reported discovery of new variable-type stars in the Galactic field. One of them was the RR Lyrae (originally discovered by Williamina Fleming), that later became an eponym for a new class of variables.

RR Lyraes are low mass (about $0.6 M_{\odot}$) and metal poor [FeH] ($0 - -2.5$ dex) stars. They are analogous to another group of pulsating variables, Cepheids. However, Cepheids are younger and more massive stars, while RR Lyrae stars are old evolved low-mass stars. They belong to spectral classes A – F with an absolute magnitude around 0.6 mag, therefore they are more than ten times more luminous than our Sun. These variables pulsate radially with periods ranging from 5 hours to 1 day and amplitudes from 0.2 to 2 mag in V-band. In various systems, mean periods, metallicities and ratio of RR Lyrae types differ, resulting in the so-called Oosterhoff dichotomy (see Sect. 1.2). A large fraction of RR Lyrae stars (according to some authors up to 50 %, see Sect. 3.2) exhibit light curve modulation known as the Blazhko effect. This astronomical field has been recently invigorated by space photometric missions, almost century-old questions enshrouding RR Lyrae variables are still unsolved and still fascinate astronomers.

1.1 Types of RR Lyrae stars

In the globular cluster ω Centauri, [Bailey \(1902\)](#) found a large number of RR Lyrae stars and divided them into three categories RRa, RRb and RRc based on their periods, amplitudes and shapes of their light curves. Stars of RRa type had the steepest rise to maximum and the largest amplitudes, RRb type stars were similar to the previous ones, but with longer periods and smaller amplitudes. The third type of RR Lyrae stars, RRc type stars, differed from the previous types. They had shorter periods and lower amplitudes with almost symmetrical light curves. A couple of decades later, [Schwarzschild \(1940\)](#) showed that stars of RRa and RRb types pulsate radially in the fundamental mode, while RRc stars pulsates in the first-overtone radial mode. A slightly modified classification of RR Lyraes is still in use.

Because RRa and RRb stars pulsate in the fundamental mode and lie in the same region of the period-amplitude diagram (sometimes called the Bailey diagram, Fig. 1.2), it is usual to combine them into a single type of RRab, alternatively called RR0. Type RRc remained unchanged since Bailey's time, but the discovery of double-mode RR Lyrae variables have expanded known RR Lyrae classes. These so-called RRd stars were identified by [Nemec \(1985\)](#). They pulsate in the fundamental and the first-overtone mode. In addition, for the other types, alternative terms RR1 for RRc, and RR01 for RRd are used. Sometimes the fourth type of RR Lyrae stars is mentioned. RRc stars are supposed to pulsate radially in the second-overtone mode, they should have

the shortest periods of all RR Lyrae stars, and a sharp peak at the maximum (Stellingwerf et al., 1987). Nevertheless, their existence is still a matter of dispute.

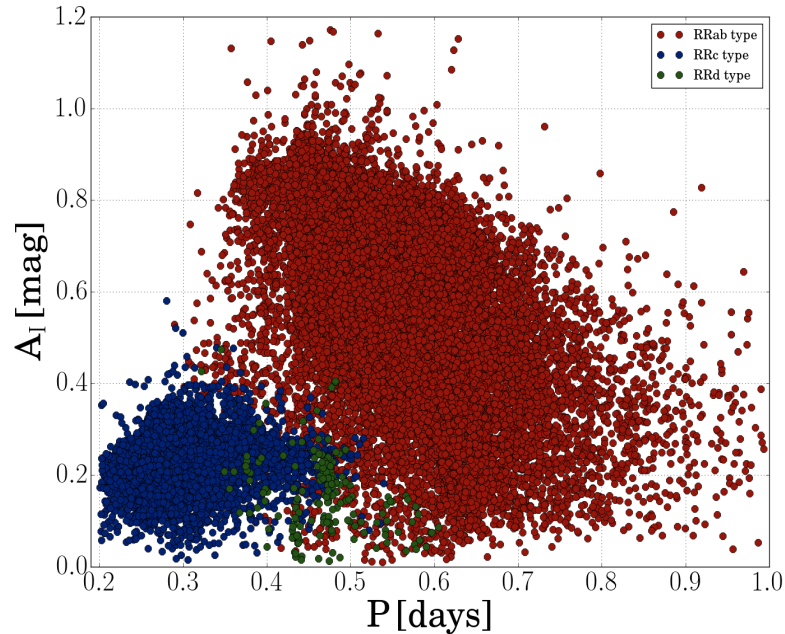


Figure 1.2: Period-Amplitude diagram for RR Lyrae stars from OGLE-IV survey (Soszyński et al., 2014).

From Fig. 1.3 we can notice that stars of RRab type have highly asymmetrical light curve in comparison with stars of other RR Lyrae subtypes. RRab stars are also easily distinguishable from other types of variable stars. Stars of RRc type (the middle panel of Fig. 1.3), on the other hand, have more symmetrical light curves, and sometimes can be misclassified as eclipsing binaries. RRd stars (the right-hand panel of Fig. 1.3), have blurry light curves due to the simultaneous pulsation in the first-overtone and the fundamental mode, where the first-overtone has usually higher amplitude than the fundamental mode.

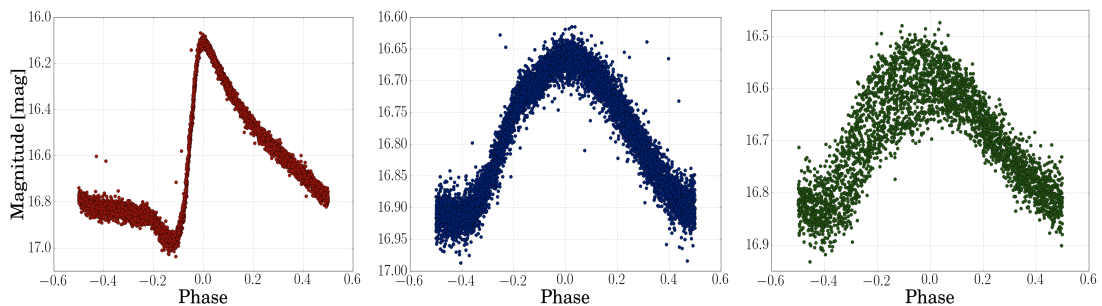


Figure 1.3: Examples of three types of RR Lyrae stars, from the left OGLE-BLG-RRLYR-06278 (RRab type), OGLE-BLG-RRLYR-06091 (RRc type), OGLE-BLG-RRLYR-09742 (RRd type) demonstrated on OGLE-IV data, Soszyński et al. (2014).

Another difference between RR Lyrae subtypes can be seen in Fig. 1.1. RRab stars (red dots) generally lie on the red edge of the instability strip in HRD. They have usually lower temperatures than RRc stars (blue dots). The first-overtone stars lie mainly, as opposed to a RRab type, on the blue edge of the instability strip of the HRD, and RRd type stars lie in the middle of the instability strip. The distribution of types of RR Lyrae variables differs from system to system, which leads to the Oosterhoff dichotomy (see Sect. 1.2). In general, approximately two-thirds of RR Lyrae stars are the RRab type (based on the VSX² catalogue, [Watson, 2006](#)).

1.2 The Oosterhoff dichotomy

During the observation of five globular clusters, [Oosterhoff \(1939\)](#) noticed a difference among RR Lyrae stars in different clusters. He suggested that globular clusters can be divided into two groups, based upon properties of RR Lyrae stars within. The two groups were later named as the Oosterhoff I and Oosterhoff II (hereafter the OoI and OoII).

The main difference between the Oosterhoff groups is in the mean pulsation periods of their RR Lyrae stars. The average period of the OoI RRab stars is $\langle P_{ab} \rangle \approx 0.55$ days, while in the OoII it is $\langle P_{ab} \rangle \approx 0.65$ days. A similar difference applies to RRc stars as well – in the OoI the mean period is $\langle P_c \rangle \approx 0.32$ days and in the OoII it is $\langle P_c \rangle \approx 0.37$ days. Another difference is in the fraction of the first-overtone pulsators, for the OoI it is approximately 17 % and for the OoII it is around 44 % ([Smith, 1995](#)).

[Sandage \(1958\)](#) proposed an explanation of the Oosterhoff dichotomy. He claimed that RR Lyrae stars in the OoII have longer periods because they are brighter than their OoI counterparts. However, this idea did not explain the difference between the OoI and OoII, but subsequently led to a period-metallicity-luminosity relation. The metallicity seems to play one of the key roles in the Oosterhoff groups, but other factors must also be taken into account. For example, the globular cluster M62, with very bright RR Lyrae stars, should belong to the OoII group, but thanks to high metal abundance, fall to the OoI group.

Normally, a globular cluster belongs to one of the two Oosterhoffs groups, but recently found globular clusters from the Large Magellanic Cloud (hereafter the LMC) seem to exhibit features from both groups. In addition, dwarf spheroidal galaxies and their globular clusters show similar attributes. Therefore they fill the so-called Oosterhoff gap and make the search for the cause of this dichotomy even more complicated ([Catelan, 2009](#)).

The Fig. 1.4 shows a distribution of globular clusters in two Oosterhoffs groups and the Oosterhoff gap. It also shows two globular clusters from the Galactic bulge and disk that fall into none of these groups. NGC 6388 and

²The International Variable Star Index

NGC 6441 form the third Oosterhoff type, and defy metallicity-luminosity relation.

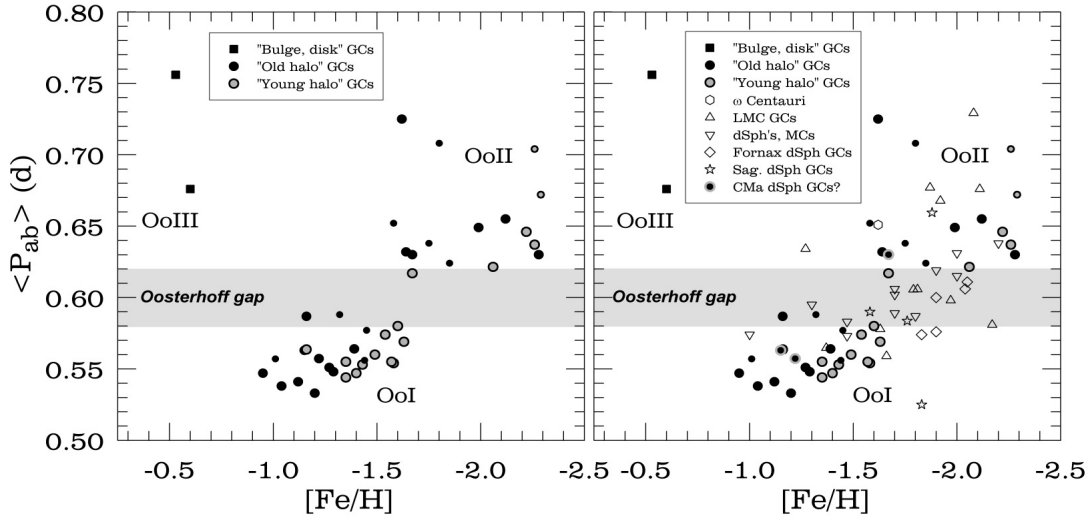


Figure 1.4: Period-metallicity dependence for different Oosterhoff groups. Galactic globular clusters are in the left-hand panel, Galactic globular clusters together with dwarf satellite galaxies and globular clusters from the LMC are in the right-hand panel (taken from [Catelan, 2009](#)).

1.3 The mechanism of pulsation

Two types of oscillation can occur in pulsating variables, radial and non-radial. Both cases result in periodical changes in shape and luminosity of a star. The main difference is that in non-radial pulsation the variations in radius are anisotropic. While some parts of stellar atmosphere move downward, others, simultaneously move upward.

Stellar pulsations can be quantified with three numbers n , l and m . The first pulsation number, n , represents radial order, and defines the order of radial pulsation. For $n = 0$ the star pulsates in the fundamental, for $n = 1$ the first-overtone mode is excited, etc. Numbers l and m describe non-radial pulsations, and specify the number of nodal lines in overall and meridian directions, respectively. Considering pulsation numbers l and m , radial pulsation is a specific example of non-radial pulsations, when the star is changing its radius keeping the spherical symmetry.

Since the discovery of the first pulsating stars, mechanism of variability had been subject to many studies. The initial hypothesis suggested binary eclipses, but it was subsequently excluded by [Shapley \(1914\)](#). One of the first who established pulsation theory was Sir [Eddington \(1918\)](#). He concluded that pulsation has to be driven by an internal mechanism within a star. In his later paper, [Eddington \(1926\)](#) proposed a so-called valve mechanism where

the valve controls the heat flow with minimum leakage. Thus, the mechanism could be considered as adiabatic.

Thirty years after Eddington's proposal, [Zhevakin \(1953\)](#) and [Cox \(1958\)](#) confirmed and elaborated the valve mechanism. In partially ionised zones, a variation in opacity κ can produce a valve. The opacity is a function of density ρ , temperature T , and parameters n and s

$$\kappa \sim \frac{\rho^n}{T^s}. \quad (1.1)$$

Outside partially ionised regions applies $n \approx 1$ and $s \approx 3.5$. During compression of such a zone the temperature and density rise, while opacity decreases. Therefore, radiation grows and a layer cannot drive the pulsation.

On the contrary, factor s decreases below zero during the compression in partially ionized regions, enlarging the opacity relatively to surrounding layers. The opacity valve is created, and radiation flow is then trapped in an ionized layer. Radiation pressure begins to build up and starts to lift the layer. As the region elevates, the atmosphere expands and starts to cool down. Cooling results in recombination, thus, diminution of opacity. Radiation flow is then released, and radiation pressure fades. Due to gravity, the layer starts its descent inwards. Free fall induces the compression of the layer, and the whole cycle starts over.

Within pulsating stars, we can find two partially ionised zones that drive the pulsations. The first zone consists of partially singly ionised hydrogen and helium (H II, He II). The second, a more inner layer, which consists mainly of twice ionised helium He III, plays the major role in driving the pulsation. The location of the two layers is crucial. For stars with the effective temperature around 7500 K, zones are close to the surface, thus do not have enough mass and density to trap the radiation flow. For cooler stars, with effective temperatures around 6500 K – 5500 K, the pulsations can be excited ([Carroll & Ostlie, 2007](#)). Among cooler stars, ionised zones are usually too deep, and the oscillation is damped. The κ mechanism is connected with the γ mechanism that serves as a support for the valve mechanism by increasing the heat capacity of the layer. Therefore enabling it to absorb more heat and increase the pressure more efficiently.

Other mechanisms that can cause pulsations are known as well. For example, the ε – mechanism is produced by variations of thermonuclear reactions rate in the core of very massive stars, or occasionally, white dwarfs. The convective blocking mechanism is caused by a threshold between convective and radiative zone. Radiative flux is repeatedly blocked at the bottom of convective zone and converted into mechanical work. This mechanism mainly applies for γ Doradus variables. The stochastically excited pulsations are driven by a turbulent motion of the stars convective zone. Modes excited by this mechanism had been detected in the Sun itself ([Catelan & Smith, 2015](#)). The study of this mechanism is one of the cornerstones of helio and asteroseismology.

1.4 Multi-mode oscillation in RR Lyraes

Multi-mode oscillations among RR Lyraes are common. Stars of RRd subclass pulsate in two modes at the same time, in the fundamental and the first-overtone. Both modes are radial and are characterized with period ratios ranging from $P_{\text{SHORT}}/P_{\text{LONG}} = 0.742 - 0.748$. The RRd stars in the Galactic bulge are somewhat an exception with period ratios starting from 0.726. The reason for this seems to be in higher metallicity in the Galactic bulge.

Thanks to the *Kepler* and COROT photometric missions, some double-mode features were discovered among RRc and RRab stars (Benkó et al., 2010; Guggenberger et al., 2012). The first-overtone, the second-overtone, and even non-radial modes were detected. So far, only modulated stars have showed additional modes. For the complete list of stars with additional periodicities from space photometric missions see Smolec (2016).

The additional modes with period ratios from 0.6 to 0.64 in RRc and RRd stars were also detected. The first detection of this additional mode was observed in AQ Leo (Gruberbauer et al., 2007). In the *Kepler* photometry 4 variables with this period ratios were identified (Moskalik et al., 2015). This field has been recently elevated by findings of Netzel et al. (2015a,b,c). They searched for radial/non-radial modes in RRc and RRd stars in OGLE-III photometry. Netzel et al. found more than one hundred RRc and RRd stars that exhibit an additional mode. They found two groups with different period ratios, the first with 0.613 and the second with 0.631. Later, they found several RRc stars forming a third group with a period ratio around 0.686. None of these period ratios corresponds to low radial modes.

To better understand the uniqueness of the newly discovered additional modes in RR Lyraes we can use the Petersen diagram (see Fig. 1.5, Petersen, 1973). This diagram originally served for estimating mass and metallicity of double-mode Cepheids. It is basically period ratio versus longer pulsation period. Today it is used not only for Cepheids, but for all kind of double or triple mode pulsators.

In Fig. 1.5, green dots stand for stars of RRd type, that pulsate in the fundamental and the first-overtone. Red dots show RRc stars with period ratio around 0.68 found by Netzel et al. (2015b) in OGLE-IV photometry. We can also notice two groups around 0.61 and 0.64, consisting of RRc and RRd stars again found by Netzel et al. (2015a,c) in OGLE-III and OGLE-IV data. The last group forming a line around 0.58 period ratio consists of stars pulsating in the fundamental and the second-overtone taken from Moskalik (2013). Stars in this group belong to RRab subtype. The additional mode that stars from this group display is the second-overtone mode.

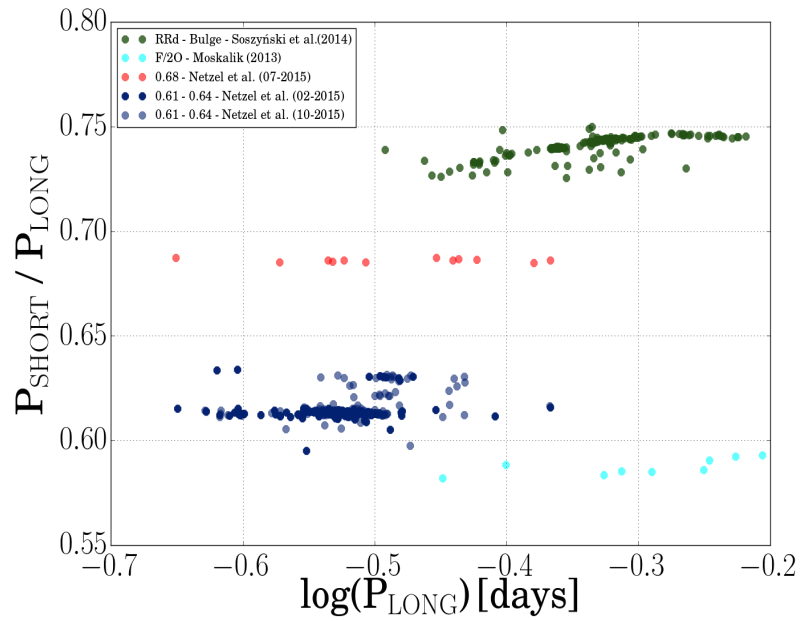


Figure 1.5: The period-Amplitude diagram for RR Lyrae stars from OGLE-IV survey (Soszyński et al., 2014).

Recently, a possible solution for stars found by Netzel et al. was suggested by Dziembowski (2015). He proposes that additional mode is caused by a non-radial fundamental mode, which is trapped in the outer layer of the envelope and is powered by the opacity mechanism.

Chapter 2

The least-squares method

THE least-squares method (hereafter LSM) is a technique commonly employed in data fitting. This method is used to describe given data using empirical or physical models. The LSM minimizes the sum of squared deviation of the data. Usually we have n number of points in pairs (t_i, y_i, σ_i) where y_i is a function of independent variable t_i (time for example) and σ_i is uncertainty of each measurement. Then model function $f(t_i, \boldsymbol{\beta})$ is used to characterize measured values. The $\boldsymbol{\beta}$ represents vector with g adjustable parameters. For given parameters the difference between measured and model values is calculated as

$$x_i = y_i - f(t_i, \boldsymbol{\beta}) . \quad (2.1)$$

Therefore, the sum of square differences is given by

$$S(\boldsymbol{\beta}) = \sum_{i=1}^n (y_i - f(t_i, \boldsymbol{\beta}))^2 . \quad (2.2)$$

The best model (minimal S) is described by a set of parameters \mathbf{b} , for which a simple condition applies

$$S(\boldsymbol{\beta} = \mathbf{b}) = \min(S) . \quad (2.3)$$

Better estimates of parameters can be achieved using weights of given y_i . The equation 2.2 can be then rewritten

$$\chi^2 = \sum_{i=1}^n (y_i - f(t_i, \boldsymbol{\beta}))^2 \cdot w_i , \quad (2.4)$$

where $w_i = \frac{1}{\sigma_i^2}$ is the weight. Based on a model function there are two approaches – a linear least-squares method (hereafter LLSM) and a non-linear least-squares method (hereafter NLLSM). To describe both we used procedures outlined in Mikulášek & Zejda (2013) and Liška (2015).

2.1 Linear least-squares method

In the LLSM, we can describe the model function f with g linear combinations of $x_i(t)$

$$f(\mathbf{x}, \boldsymbol{\beta}) = \sum_{i=1}^g \beta_i x_i = \mathbf{x}\boldsymbol{\beta} , \quad (2.5)$$

the \mathbf{x} is a vector function of time

$$\mathbf{x} = (x_1, x_2, \dots, x_g) = \left(\frac{\partial f}{\partial \beta_1}, \frac{\partial f}{\partial \beta_2}, \dots, \frac{\partial f}{\partial \beta_g} \right) = \vec{\nabla} f(t, \boldsymbol{\beta}) . \quad (2.6)$$

For clarity, it is better to write the previous relation in matrix notation

$$\mathbf{y} = \begin{pmatrix} y_1 \\ y_2 \\ \vdots \\ y_n \end{pmatrix} , \quad \mathbf{X} = \begin{pmatrix} x_{11} & x_{12} & \cdots & x_{1g} \\ x_{21} & x_{22} & \cdots & x_{2g} \\ \vdots & \vdots & \ddots & \vdots \\ x_{n1} & x_{n2} & \cdots & x_{ng} \end{pmatrix} = \begin{pmatrix} \mathbf{x}_1 \\ \mathbf{x}_2 \\ \vdots \\ \mathbf{x}_n \end{pmatrix} . \quad (2.7)$$

The \mathbf{y} is a column vector filled with n number of observations, \mathbf{X} is a matrix with size $n \times g$ containing function values x_{ik} . Further, we can define other matrices as

$$\mathbf{f}(\mathbf{X}, \boldsymbol{\beta}) = \begin{pmatrix} f_1 \\ f_2 \\ \vdots \\ f_n \end{pmatrix} = \begin{pmatrix} \mathbf{x}_1 \\ \mathbf{x}_2 \\ \vdots \\ \mathbf{x}_n \end{pmatrix} \cdot \boldsymbol{\beta} = \mathbf{X} \cdot \boldsymbol{\beta} , \quad \mathbf{W} = \begin{pmatrix} w_1 & 0 & \cdots & 0 \\ 0 & w_2 & \cdots & 0 \\ \vdots & \vdots & \ddots & \vdots \\ 0 & 0 & \cdots & w_n \end{pmatrix} . \quad (2.8)$$

The diagonal matrix \mathbf{W} consists of weights of measurements. The final solution of LLSM using matrix formalism is then

$$\mathbf{U} = \mathbf{X}^T \cdot \mathbf{W} \cdot \mathbf{y} , \quad \mathbf{V} = \mathbf{X}^T \cdot \mathbf{W} \cdot \mathbf{X} , \quad \mathbf{H} = \mathbf{V}^{-1} , \quad (2.9)$$

where \mathbf{U} is a vector, \mathbf{V} is a $g \times g$ matrix and \mathbf{H} is a covariant matrix. For \mathbf{b} , \mathbf{y}_p and χ^2 applies

$$\mathbf{b} = \mathbf{H} \cdot \mathbf{U} , \quad \mathbf{y}_p = \mathbf{X} \cdot \mathbf{b} , \quad \chi^2 = \mathbf{y}^T \cdot \mathbf{W} \cdot \mathbf{y} - \mathbf{b}^T \cdot \mathbf{U} . \quad (2.10)$$

To determine uncertainties of parameters of model \mathbf{b} and estimates of model function \mathbf{y}_p , we use following relations

$$\delta \mathbf{y}_p = \sqrt{\chi_R^2 \text{diag}(\mathbf{X} \cdot \mathbf{H} \cdot \mathbf{X}^T)} , \quad \delta \mathbf{b} = \sqrt{\chi_R^2 \text{diag}(\mathbf{H})} . \quad (2.11)$$

The variable χ_R^2 is a dimensionless variable connected with χ^2 via equation

$$\chi_R^2 = \frac{\chi^2}{n-g} . \quad (2.12)$$

The χ_R^2 depends on used model and should vary around one. In LLSM a linear model function has only one minimum, the best parameters are components of vector \mathbf{b} .

2.2 Non-linear least-squares method

Generally, we are unable to use the model function as a linear combination of g independent variables. Therefore, we cannot use LLSM, but we have to use NLLSM. Using this method we usually try to transform non-linear model to a linear one using Taylor expansion of the first order

$$f(\mathbf{b}_0, \Delta\boldsymbol{\beta}) \cong f(\mathbf{b}_0) + \sum_{k=1}^g \Delta\beta_k \frac{\partial f(\mathbf{b}_0)}{\partial \beta_k} = f(\mathbf{b}_0) + \Delta\boldsymbol{\beta}\mathbf{x} . \quad (2.13)$$

For NLLSM we can rewrite equation 2.2 into this form

$$\chi^2(\boldsymbol{\beta}) = \sum_{i=1}^n [y_i - f(x_i, \boldsymbol{\beta}) - \Delta\boldsymbol{\beta}\mathbf{x}]^2 , \quad (2.14)$$

$$\chi^2 = \sum_{i=1}^n [\Delta y - \Delta\boldsymbol{\beta}\mathbf{x}]^2 . \quad (2.15)$$

This equation can be transformed using a matrix notation (including weights) as

$$\left(\mathbf{X}^T\mathbf{W}\mathbf{X}\right)\Delta\mathbf{b} = \mathbf{X}^T\mathbf{W}\Delta\mathbf{y} . \quad (2.16)$$

Consequently we proceed similarly as in the case of LLSM

$$\mathbf{x} = (x_1, \dots, x_g)^T = \left(\frac{\partial f(\mathbf{b}_0)}{\partial \beta_1}, \frac{\partial f(\mathbf{b}_0)}{\partial \beta_2}, \dots, \frac{\partial f(\mathbf{b}_0)}{\partial \beta_g} \right)^T . \quad (2.17)$$

The \mathbf{x} and \mathbf{b}_0 are vectors, where \mathbf{b}_0 contains a guess of initials parameters. Matrices \mathbf{X} and \mathbf{W} are more or less similar to the LLSM case, and the solution of NLLSM in matrix formalism looks like this

$$\Delta\mathbf{y} = \mathbf{y} - f(\mathbf{b}_0) , \quad \Delta\mathbf{b} = \left(\mathbf{X}^T\mathbf{W}\mathbf{X}\right)^{-1} \mathbf{X}^T\mathbf{W}\Delta\mathbf{y} \quad (2.18)$$

$$\mathbf{U} = \mathbf{X}^T\mathbf{W}\Delta\mathbf{y} , \quad \mathbf{V} = \mathbf{X}^T\mathbf{W}\mathbf{X} , \quad \mathbf{H} = \mathbf{V}^{-1} . \quad (2.19)$$

At the beginning of the calculation, we have to estimate the initial parameters \mathbf{b}_0 . After the first iteration, we add values of $\Delta\mathbf{b}$ with respect to \mathbf{b}_0 , and use this value as a new estimate. This process is repeated several times until we reach desired precision. To determine the errors of our parameters we use analogous relations as in LLSM

$$\chi_R^2 = \frac{\chi^2}{n-g} , \quad \delta\mathbf{b} = \chi_R \sqrt{\text{diag}(\mathbf{H})} . \quad (2.20)$$

2.2.1 Levenberg–Marquardt algorithm

This method was for the first time proposed by [Levenberg \(1944\)](#), and later improved by [Marquardt \(1963\)](#). It provides a fast solution to a non-linear least-squares problem. We again start with relation [2.2](#) and work our way up to the equation [2.16](#). [Levenberg](#) proposed damped version of equation [2.16](#)

$$\left(\mathbf{X}^T\mathbf{W}\mathbf{X} + \lambda\mathbf{I}\right)\Delta\mathbf{b} = \mathbf{X}^T\mathbf{W}\Delta\mathbf{y} . \quad (2.21)$$

In this relation, \mathbf{I} is an identity matrix and λ is a positive damping factor. The parameter λ is improved in each iteration. If the new approximation is better than the previous one, λ decreases and vice versa. The problem with this approach is when λ is too large in comparison with Hessian matrix $\mathbf{X}^T\mathbf{W}\mathbf{X}$. A solution to this problem was proposed by [Marquardt](#), who employed diagonal elements of $\mathbf{X}^T\mathbf{W}\mathbf{X}$ instead of identity matrix \mathbf{I}

$$\left[\mathbf{X}^T\mathbf{W}\mathbf{X} + \lambda \left(\mathbf{X}^T\mathbf{W}\mathbf{X}\right)\right]\Delta\mathbf{b} = \mathbf{X}^T\mathbf{W}\Delta\mathbf{y} . \quad (2.22)$$

2.2.2 Trigonometric polynomial

We will apply NLLSM to a trigonometric polynomial (so-called Fourier series eq. [2.23](#)), which is often used to describe light curves of pulsating stars (see also Sect. [2.3](#))

$$m(t) = A_0 + \sum_{i=1}^N A_i \sin(2i\pi\vartheta(t) + \varphi_i) . \quad (2.23)$$

In this formula, φ_i are phase shifts, A_i are amplitudes, and N is a degree of the polynomial. The $\vartheta(t)$ is the phase function, which can be expressed as

$$\vartheta(t) = \frac{t - M_0}{P} , \quad (2.24)$$

where M_0 is the zero epoch, in pulsating stars usually the time of maximum brightness, P is a period and t is a time of observation. Using equation [2.17](#) we can derive components \mathbf{x} of matrix \mathbf{X}

$$\mathbf{x} = \left(\frac{\partial m(t)}{\partial a_0}, \dots, \frac{\partial m(t)}{\partial a_N}, \frac{\partial m(t)}{\partial \varphi_1}, \dots, \frac{\partial m(t)}{\partial \varphi_N}, \frac{\partial m(t)}{\partial M_0}, \frac{\partial m(t)}{\partial P} \right) . \quad (2.25)$$

Decision, which parameters are fixed and which should be adjusted by the NLLSM, is somewhat arbitrary and depends on the application.

The essential problem of using trigonometric polynomials is how to determine the degree of the fit n . For highly asymmetrical and crooked light curves of the RRab subtype it is usually necessary to use high order of polynomial. The final decision should be based on the quality of the data. If we have a long sample with good phase coverage, we can use higher-order equation [2.23](#).

To estimate the most appropriate degree of a fit, information criteria can be applied. For example, Bayesian information criterion

$$BIC = \chi^2 + g \cdot \ln n , \quad (2.26)$$

or Akaike criterion

$$AIC = \chi^2 + 2 \cdot g . \quad (2.27)$$

The variable g is a number of parameters and n is a number of data points. To determine the appropriate degree of polynomial, we need to calculate several models for different orders. The model with the smallest information criteria is then considered to be the most appropriate.

Ultimately higher degree of the trigonometric polynomial does not always mean more appropriate fit as we can see in plots in Fig. 2.1. Both stars have approximately the same number of data points, while the precision of the fit differs significantly. For both stars, we used the tenth and the sixth order of the polynomial. While for the star on the right-hand side panels the fit differs only slightly for different degree of the polynomial, in the left-hand panels it improved greatly with lower order of the fit. One needs to be cautious when deciding what degree of polynomial should be used.

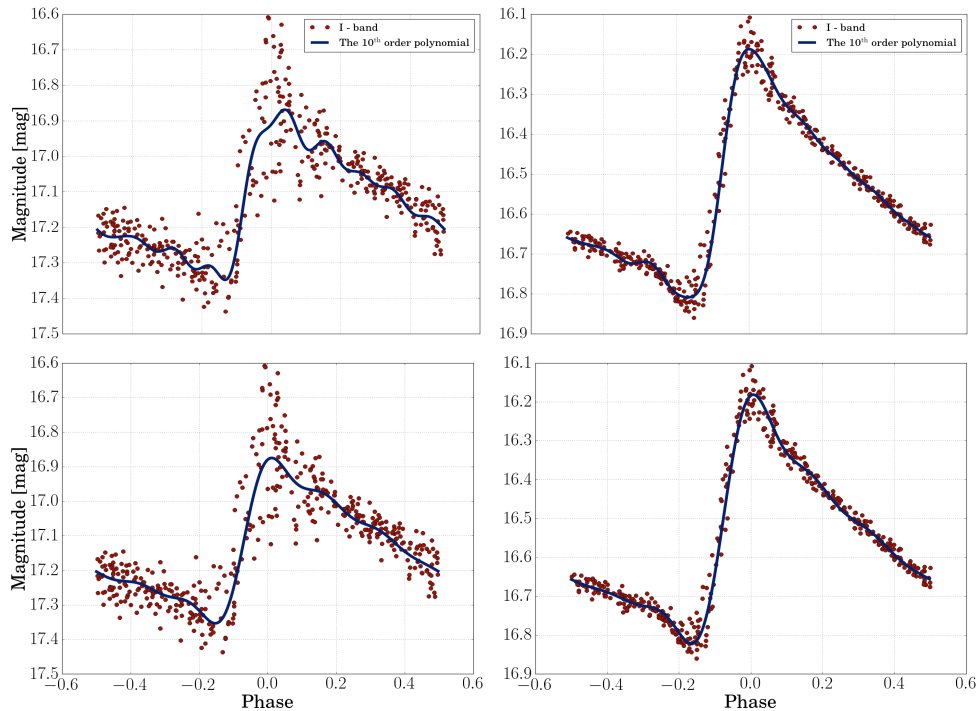


Figure 2.1: An example of different degrees of trigonometric polynomial fit for OGLE-BLG-RRLYR-01237 (left-hand panels) and OGLE-BLG-RRLYR-01254 (right-hand panels). The top panels shows two examples of tenth degree polynomial fit, while the bottom panels show the sixth order fits. Data were acquired from OGLE-IV, [Soszyński et al. \(2014\)](#).

2.3 The Fourier coefficients

The light curves of RR Lyrae stars can be described using a finite number of sines (see eq. 2.23). This technique was used for the first time by [Simon & Lee \(1981\)](#) to study Cepheids. Later on, this method was used to analyse light curves of RR Lyrae stars ([Simon, 1988](#)). Using Fourier parameters A_i and φ_i we can derive amplitude ratios R_{i1} and differences in phase φ_{i1} as follows

$$R_{i1} = \frac{A_i}{A_1} , \quad (2.28)$$

$$\varphi_{i1} = \varphi_i - i\varphi_1 . \quad (2.29)$$

These Fourier coefficients serve as indicators of physical parameters and variability type. In both panels of Fig. 2.2, we see an apparent difference between RRc and RRab stars regarding their Fourier coefficients R_{31} and φ_{31} . The most importantly, Fourier parameters can be used for estimation of physical parameters of RR Lyrae stars ([Jurcsik & Kovacs, 1996](#); [Jurcsik, 1998](#)). The parameters φ_{21} and φ_{31} are often used to determine metallicity. Through metallicity, we can derive other parameters, such as effective temperature T_{eff} , mass M , absolute magnitude M_V , and others.

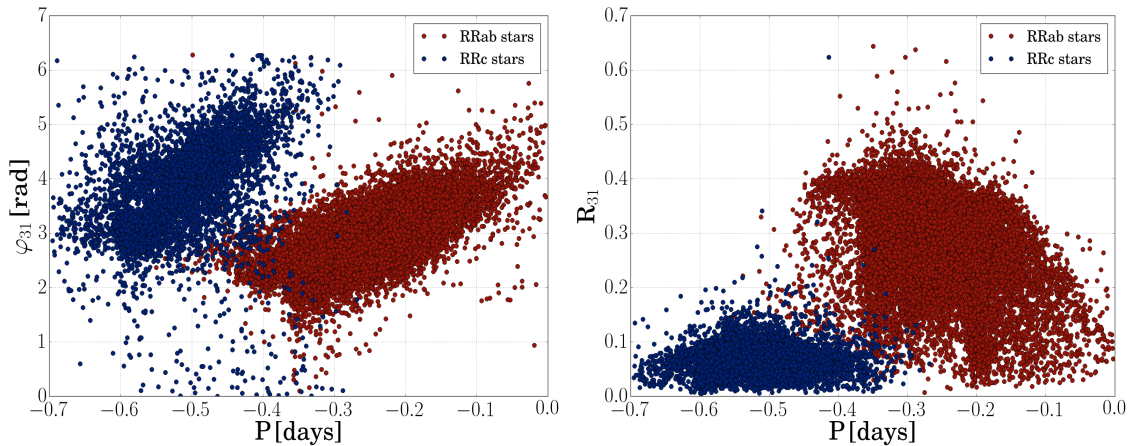


Figure 2.2: Fourier coefficients for RRab and RRc stars. The left-hand figure shows period- φ_{31} , while the right-hand plot displays period- R_{31} dependence. Demonstrated on OGLE-IV data, [Soszyński et al. \(2014\)](#).

Chapter 3

The Blazhko effect

ONE of the long-lasting mysteries in RR Lyraes is the Blazhko effect, a quasi-periodic modulation of the light curve. Despite breakthroughs achieved by space photometric missions, the Blazhko puzzle still remains unsolved.

The Blazhko effect was discovered by [Sergei N. Blažko \(1907\)](#), and is named after this Russian astronomer. During his observation of RW Dra he noticed irregularities in the times of maxima, which were later explained as phase modulation. Several years later, [Shapley \(1916\)](#) reported cyclic variations in an amplitude of the prototype star RR Lyrae itself, uncovering the amplitude modulation.

The amplitude modulation is not only a domain of RR Lyrae stars, but it also occurs among different types of variables. For example, some of the first and the second-overtone Cepheids in the LMC show similar behaviour ([Moskalik & Kołaczkowski, 2009](#)). However, the Blazhko effect among RR Lyrae stars still stands out for several reasons. First of all, both amplitude and phase modulations seem to be present in modulated RRab stars ([Benkő et al., 2010](#)). Furthermore, the occurrence of stars exhibiting the Blazhko effect can be as high as 50% (e.g. [Jurcsik et al., 2014](#)). Lastly, the discovery of the *period doubling* (hereafter PD, [Szabó et al., 2010](#)) accompanying the Blazhko effect emphasizes the peculiarity of this phenomenon among RR Lyrae stars.

The period of modulation does not always remain constant, variations in modulation are observed, hence, the Blazhko effect is considered to be quasiperiodic. One example for all is the RR Lyrae star itself, where the Blazhko modulation vanished and reappeared over the years ([Poretti et al., 2016](#)). The length of the Blazhko cycle differs from star to star, within the interval from several days up to several years. The shortest known modulation period does not drop below 5 days ([Skarka, 2013](#)). Finding the longest Blazhko periods depends strongly on the time span of the data (hereafter referred to as *TS*). The possible Blazhko periods comparable to the *TS*, can as a matter of fact be just long-term period changes. On the other hand, the Blazhko modulation with a period more than 25 years was reported ([Jurcsik & Smitola, 2016](#)).

An example of the diversity of the Blazhko effect can be seen in figure 3.1. All six plots show stars with the Blazhko effect, that are distributed according to the strength of amplitude modulation. The top figures display stars with almost no amplitude modulation, the middle show stars with medium amplitude modulation, and the bottom panels show stars with strong amplitude modulation.

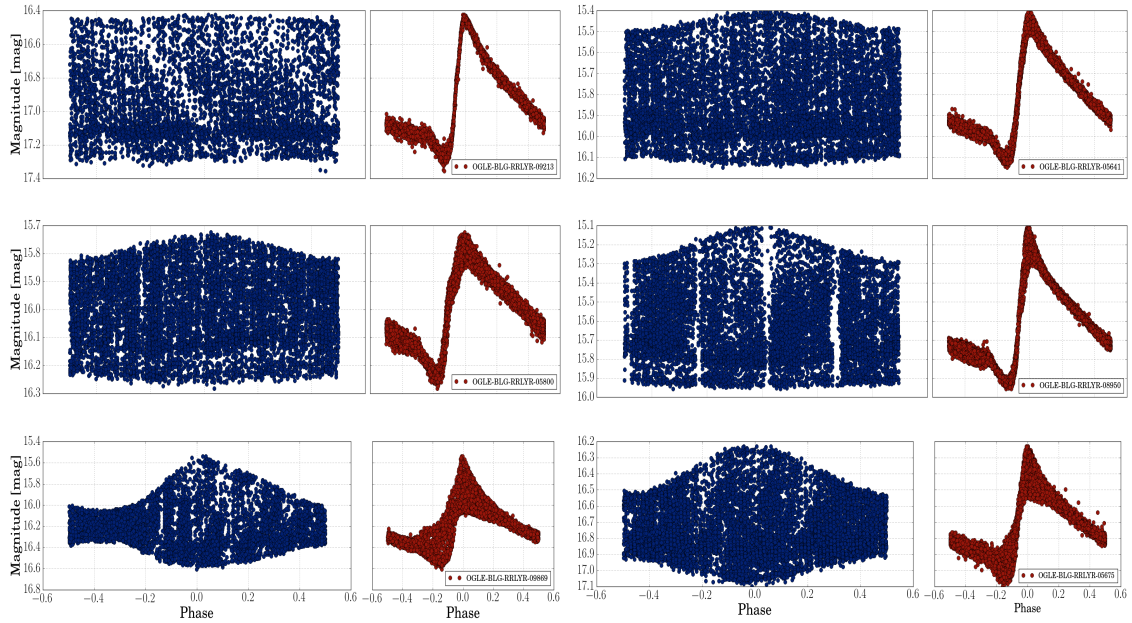


Figure 3.1: The demonstration of heterogeneity of the Blazhko effect, sorted by the distinctiveness of amplitude modulation. Data from OGLE-IV, [Soszyński et al. \(2014\)](#).

3.1 Frequency spectra of RR Lyrae stars

In RR Lyrae stars with stable light curve, the frequency spectrum contain a peak for the basic pulsation frequency and integer multipliers of this peak. Space photometric observations can be continuous and ultra precise, with clear frequency spectra with peaks for the main pulsation frequency and its harmonics (for stable stars). Ground-based measurements can be somewhat limited, resulting in contamination of frequency spectrum with additional peaks (even for stable stars). These peaks are spaced mainly either with a one-day, or yearly rate (depending on the periodicity of observations). The reason for these aliases are day and night cycles and a limited observation during the years. The Fig. 3.2 shows a spectrum of a RRab type star from ground-based observation. We can see the main pulsation frequency f_0 with daily aliases $f_0 \pm k$, where k is integer, and additional peaks related to harmonics kf_0 .

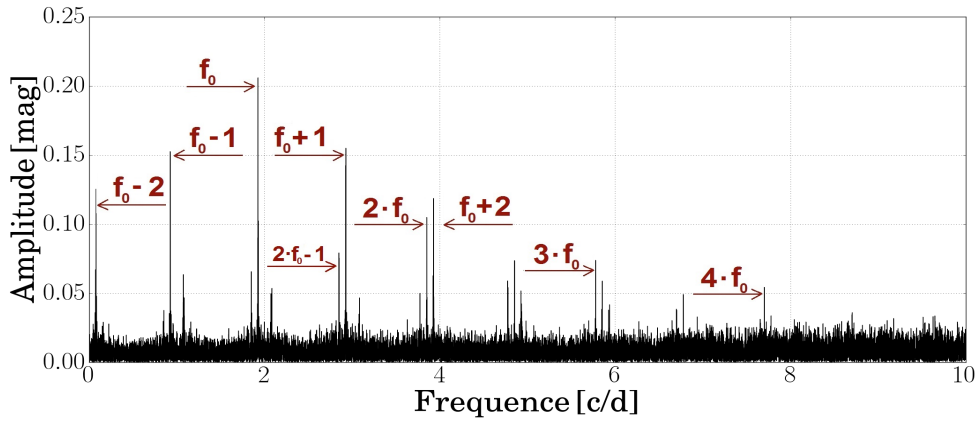


Figure 3.2: The frequency spectrum of a modulated RR Lyrae star (OGLE-BLG-RRLYR-04415) with the basic pulsation frequency, its four harmonics, and respective aliases. Data taken from OGLE-IV survey (Soszyński et al., 2014).

In the frequency domain, the Blazhko effect manifests itself in diverse forms of equidistant peaks in vicinity of the main pulsation frequency and its harmonics. The Blazhko stars frequency spectrum can contain one side frequency peaks (doublets), or symmetrical side peaks (triplets). Sometimes even quintuplets and septuplets are detected from ground based observations. Theoretically, we can find infinite number of side peaks, in some special cases.

In addition, sometimes we can detect even the Blazhko frequency itself, but finding such frequency is complicated and limited for certain cases of the Blazhko modulation. The peak for Blazhko frequency have often low amplitude and sometimes can be hidden in the noise. Furthermore, the peak for such frequency can be found only when the amplitude modulation is asymmetric. Thus, for identification of the Blazhko effect, it is easier to look at the close vicinity of the main pulsation frequency and its harmonics.

The following relationships and labelling have been taken from Benkó et al. (2011). The amplitude modulation can be mathematically expressed using sine function similar to 2.23 with an additional component

$$U_{AM}(t) = [U_c + U_m(t)] \cdot \sin(2\pi f_c t + \varphi_c) , \quad (3.1)$$

$$U_m(t) = U_m^A \cdot \sin(2\pi f_m t + \varphi_m^A) , \quad (3.2)$$

$$U_{AM}(t) = U_c \sin(2\pi f_c t + \varphi_c) + \frac{U_m^A}{2} \{ \sin[2\pi(f_c - f_m)t + \varphi^-] + \sin[2\pi(f_c + f_m)t + \varphi^+] \} . \quad (3.3)$$

Equation 3.1 represents a wave with additional signal U_m that varies the original amplitude U_c . The second equation 3.2 express the assumed modulated (sinusoidal) signal, and the last equation wraps it all together. We should take notice that the second part of the equation 3.3 shows positive and negative f_m . This represents Blazhko frequency and gives rise to a triplet components in a frequency spectrum.

The phase and frequency modulation is impossible to distinguish without any additional hint. The frequency modulation can be described using sine

function again

$$U_{\text{FM}}(t) = U_c \sin [2\pi f_c t + 2\pi k_{\text{FM}} U_m^{\text{F}}(t) + \varphi_c] , \quad (3.4)$$

$$U_m^{\text{F}}(t) = \frac{U_m^{\text{F}}}{2\pi f_m} \sin(2\pi f_m t + \varphi_{\text{F}}^{\text{m}}) , \quad (3.5)$$

$$U_{\text{FM}}(t) = U_c \sin [2\pi f_c t + \eta \sin(2\pi f_m t + \varphi_{\text{m}}^{\text{F}}) + \varphi_c] . \quad (3.6)$$

The variable η stands for modulation index and is defined as

$$\eta = \frac{k_{\text{FM}} \cdot U_m^{\text{F}}}{f_m} . \quad (3.7)$$

We have a sinusoidal signal U_m^{F} that modulates the original signal U_{FM} with modulation frequency f_m .

Stars can also exhibit more than one Blazhko modulation. There are well-known examples of stars with two, or even three Blazhko periods, for instance, RS Boo (see the online version of the list by [Skarka \(2013\)¹](#)). Supplementary equidistant peaks represent additional multiple modulating frequencies. Each modulation frequency has a different length and effect on phase curve. Based on the observation by *Kepler* space telescope, it seems that the vast majority of the Blazhko stars manifest several modulation periodicities (around 80%, [Benkő et al., 2014](#)).

The amplitudes of modulation peaks are generally asymmetric, sometimes even with one side peak under the detection limit. The vast majority of modulated stars have dominant peak at the right-hand side of the main pulsation frequency and its harmonics ([Alcock et al., 2003](#)). This behavior is a consequence of a difference in phase between phase and amplitude modulation ([Benkő et al., 2011](#)).

Another interesting feature of RR Lyrae stars had been found thanks to the space photometric missions. The *Kepler* space telescope revealed, for the first time among RR Lyrae stars, PD phenomenon which can be identified in Fourier spectrum as peaks with half-integer frequencies between the basic pulsation frequency and its harmonics ([Szabó et al., 2010](#)). Therefore obtaining full light curve solution (identifying all present frequency peaks) of RR Lyrae stars is complicated.

Both plots in Fig. 3.3 show the close vicinity of main pulsation frequency of modulated star, same star as in the Fig. 3.2. The left-hand plot in Fig. 3.3 shows the basic pulsation frequency and alias from the first harmonic. The right-hand plot in the same figure displays the Blazhko modulation peaks after removing the basic pulsation frequency (shown with the red line) and several harmonics. We can see an equidistant triplet structure with unequal amplitudes.

¹Known Blazhko stars in Galactic field, <http://www.physics.muni.cz/~blasgalf/>

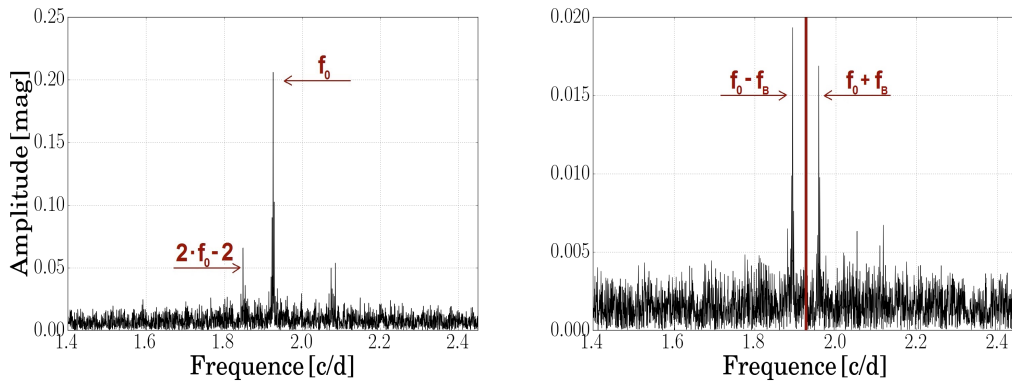


Figure 3.3: Close vicinity of the basic pulsation frequency of modulated star, same star as in Fig. 3.2. The left-hand panel shows the frequency spectrum with the main pulsation frequency. The right-hand panel shows two equidistant peaks produced by the Blazhko modulation after we removed the basic pulsation frequency (red line).

3.2 The occurrence of the Blazhko effect

The Blazhko phenomenon does not concern only RRab subtype, examples of modulation among RRC and RRd subtypes are also known. TV Boo is one of a few RRC type stars showing the Blazhko effect with a period of modulation of 9.7374 days (Skarka & Zejda, 2013). Among double-mode RR Lyrae stars, there are at least 15 known cases, where one, or both modes exert the Blazhko modulation (Smolec et al., 2015).

The estimates of an incidence rate of the Blazhko effect among RR Lyrae stars have changed significantly during the past years. Recently, thanks to the space photometric surveys, the fraction of modulated stars seems to be approximately 50%. The occurrence differs among different stellar systems, depending on available data, and according to the method of detection. Szeidl (1976) gave the first estimate of the incidence rate of the Blazhko stars as 15–20%. At the beginning of a new millennium, using large ground-base sky surveys, Szczygieł & Fabrycky (2007) reported a significantly lower ratio, approximately 5%. On the other hand, Jurcsik et al. (2009) reported 47% fraction of the Blazhko stars. Similar result reported Benkő et al. (2010) 48%, from *Kepler* space photometric mission. Therefore, the lower fraction found by Szczygieł & Fabrycky (2007) is most likely caused by the poor quality of the data.

A number of the Blazhko stars in comparison to the unmodulated stars outside our Galaxy appears to be slightly lower, for the LMC it is about 20% (Soszyński et al., 2009) and 22% for the Small Magellanic Cloud² (Soszyński et al., 2010). Globular clusters, on the other hand, show large number of modulated stars, e.g. 50% in M3 (Jurcsik et al., 2014) and 46% in M53 (Ferro et al., 2012). This different fraction of the Blazhko stars for the Galactic and extragalactic systems raises the question of what is the cause of this inhom-

²hereafter referred to as the SMC

geneity. One of the reasons could be different physical properties of RR Lyrae stars, or quality of the data. For a short list of percentage of Blazhko stars in various stellar systems see tab. 3.1.

Table 3.1: The percentage of the Blazhko RRab stars in different stellar systems, with affiliation to Oosterhoff groups for globular clusters and total number of RRab stars in each system.

Stellar system	% percentage	# number of stars	Authors
Galactic field	47 %	30	Jurcsik et al. (2009)
	48 %	29	Benkó et al. (2010)
M3 (OoI)	50 %	200	Jurcsik et al. (2014)
M5 (OoI)	36 %	50	Jurcsik et al. (2011)
M53 (OoII)	46 %	24	Ferro et al. (2012)
LMC	20 %	17 693	Soszyński et al. (2009)
SMC	22 %	1 933	Soszyński et al. (2010)
Galactic bulge	30%	11 756	Soszyński et al. (2011)

3.3 The length of the Blazhko modulation

Periods of the Blazhko modulation vary from a couple of days up to several years. The limit for the longest Blazhko effect is unknown, due to a lack of long-term precise observation. Another issue with long period Blazhko effect is changes in the period that can mimic the Blazhko modulation. The vast majority Blazhko periods falls into interval from 30 to 120 days (Skarka et al., 2016).

No direct connection between the Blazhko modulation and pulsation period is known, but Jurcsik et al. (2005) determined minimal value of a modulation frequency at a given primary pulsation frequency as

$$f_{\text{MAX_BLAZHKO}} = 0.125 \cdot f_0 - 0.142 . \quad (3.8)$$

The $f_{\text{MAX_BLAZHKO}}$ is the highest Blazhko frequency for a given main pulsation frequency f_0 . This relation implies that short periodic RR Lyrae stars can have both short or long light curve modulation, while RR Lyrae variables with long pulsation periods tend to have longer Blazhko periods.

On longer time scales we can study irregularities in Blazhko periods. One example is the RR Lyrae itself, where the Blazhko effect disappears and reappears with a four-year periodicity. The length of the modulation cycle in the RR Lyrae varies between 38 – 41 days (Le Borgne et al., 2014), thus, the star exhibits quasi-periodic variation. In addition, changes in Blazhko periods are sometimes accompanied by an alteration in pulsation period. Variance in both periods can be discordant or concordant.

3.4 Differences between modulated and unmodulated stars

Besides obvious differences in the frequency spectrum, and often in the appearance of phase curves, several differences between the Blazhko stars and unmodulated stars have been found.

Szeidl (1988) showed that amplitudes of the Blazhko stars fit the group of the monophasic stars only when they are in the brightest point of the Blazhko cycle. Therefore, the Blazhko effect is probably a suppressing phenomena. Later, Alcock et al. (2003) in their study of RR Lyrae stars in the LMC found that overall amplitudes for modulated stars tend to be smaller than for stable counterparts. Therefore, they confirmed Szeidl (1988) findings.

They also calculated Fourier parameters for studied stars and discovered significantly higher amplitudes for higher order Fourier coefficients in unmodulated stars. Hence, stars with the Blazhko effect have lower amplitudes and smaller skewness.

The question whether modulated stars have shorter periods remains unsolved. Moskalik & Poretti (2003) reported that the Blazhko stars in the Galactic bulge show no difference in pulsation periods, in comparison with their stable counterparts. In globular cluster M5, Jurcsik et al. (2011) stated that multi-periodic stars have shorter periods by a factor 0.04 days in comparison with all RRab stars in M5. Somewhat in contrary to their findings, Skarka (2014b) reported only a very small difference in periods between Blazhko and non-Blazhko stars in the Galactic field.

The difference in absolute magnitudes of stable and modulated stars is unclear. Jurcsik et al. (2011) found that the Blazhko stars are slightly fainter (approximately of $\Delta M_V = 0.05$ mag) compared to unmodulated stars. Similar difference was found by Skarka (2014b) in his study of Galactic field stars. While studying RR Lyrae stars in M53, Ferro et al. (2012) found no difference in absolute magnitudes. Thus, Ferro et al. (2012) proposed evolutionary character of the Blazhko effect. Gillet et al. (2013) used data from the *Kepler* space telescope to construct HRD and found that the Blazhko stars are hotter in contrast with stable stars. Due to a small number of used stars, this result could be an observational bias. In addition, Skarka (2014b) did not report any difference in temperature between modulated and unmodulated stars.

Some RR Lyrae pulsators undergo either positive or negative change in period. Vandenbroere et al. (2012) suggests that period change occurs more frequently among modulated stars. Whether changes in periods of the Blazhko stars have increasing or decreasing tendency, is unclear. The globular cluster M5 exhibits opposite period irregularities for modulated stars than modulated stars in the Galactic field (Jurcsik et al., 2012).

The possibility of connection between the Blazhko effect and metallicity is unconfirmed. In the past, several different results had been reported. Szeidl (1976), using spectroscopic metallicity, suggested that modulated stars have slightly lower metallicity. Opposite results were reported by Moskalik & Poretti

(2003) for stars in the Galactic bulge using photometric data. In addition, Smolec (2005) found no connection between metallicity and the Blazhko effect in the LMC and the Galactic bulge. The same results were obtained by Skarka (2014b) in his study of the Galactic field stars.

3.5 Physical models of the Blazhko effect and period doubling

Since its discovery, many scientists tried to explain the Blazhko effect without clear success. One of the most promising models of the Blazhko modulation was *Non-Radial Resonant Rotator/Pulsator*, in which non-linear interaction between non-radial and radial modes was assumed (Van Hoolst et al., 1998). Another model is *Magnetic Oblique Rotator/Pulsator*, which assumes that a star has a strong magnetic field which causes deformation of otherwise radial pulsations (Shibahashi, 2000). Both models expect symmetric modulation components, therefore, the opposite of what we see in frequency spectrum in most of the stars with the Blazhko modulation.

New efforts to explain the Blazhko phenomena were invigorated by the detection of PD in data from the *Kepler* mission. Majority of the Blazhko stars from the *Kepler* field exhibited PD in contrast with unmodulated stars that showed no signs of maxima alternations. Therefore, a strong connection with the Blazhko effect is probable. Solution to the PD was outlined by Kolláth et al. (2011) as a 9:2 resonance between the fundamental mode and higher-order radial overtone (most likely 9th). Later, Buchler & Kolláth (2011) suggested that the resonance 9:2 could be responsible for the Blazhko effect. They based their conclusion on amplitude equations, and, in addition, their model can generate quasiperiodic modulation. Similar resonance, 3:2, can produce a modulation in models of BL Her stars (Smolec & Moskalik, 2012). Their findings were concluded from hydrodynamic simulations. Furthermore, Gillet (2013) outlined the *Shock wave model*, in which the fundamental and the first-overtone are excited, and cause shock waves in the atmosphere that induce the Blazhko effect. Lastly, the *Hybrid model*, proposed by Bryant (2014), is based on an interaction of the fundamental and the first-overtone, where one of the components is sinusoidal, while the other one is highly non-sinusoidal. However, this model does not reproduce the PD. Despite recent progress in understanding the Blazhko effect, there is still a lot of work to be done.

Chapter 4

OGLE survey and data acquisition

THE Optical Gravitational Lensing Experiment (OGLE, [Udalski et al. \(1992\)](#), [Udalski et al. \(2015\)](#)) is an ongoing long-term experiment managed by University of Warsaw, Poland. The beginnings of this project reach back to the end of the 20th century. The OGLE was one of the first projects aimed to search for microlensing events caused by proposed dark matter in the Galactic halo. Its original focus slightly shifted from gravitational lensing to sky variability in recent years.

In more than two decades, OGLE have evolved substantially. The first stage OGLE-I started at the Las Campanas Observatory in Chile in 1992 with Swope telescope (1.0 m in diameter) using single-chip CCD camera. At this season, only the Galactic bulge was observed due to limited telescope access. OGLE-II began in 1997 with 1.3 m Ritchey-Chrétien telescope equipped with new, but still single-chip CCD camera. Thanks to the unlimited access to the telescope, new targets were added (the LMC and SMC). The third phase initiated in summer 2001 with the same telescope, with a new camera with eight CCDs chips arranged in a mosaic, was acquired. Difference Image Analysis technique was implemented for image processing ([Alard & Lupton, 1998](#); [Alard, 2000](#); [Wozniak, 2000](#)). Significant hardware upgrade took place in 2010 with a new 262.5 megapixel 32-chip mosaic CCD camera, which covers the entire field of view of the telescope, meaning the beginning of the era of OGLE-IV survey ([Soszyński et al., 2014](#)). New *V* and *I* band filters were designed and manufactured. While *V* filter is rather different from the standard Johnson *V* filter, filter *I* is quite similar to its counterpart from the standard Kron-Cousins system. The whole set up allows to reach 100% completeness up to 19 mag in *I* for lower stellar density fields, and 18.5 mag in the highest stellar density fields.

4.1 OGLE-IV

The latest season of OGLE mission was completed in October 2013 (with a small exception for sparsely observed fields). During its four-year run, millions of stars were observed in the LMC and SMC, Galactic disk and the Galactic bulge, including many variable objects. [Soszyński et al. \(2014\)](#) published a catalogue containing over 38 000 RR Lyrae stars (more than one-third of known RR Lyrae variables), making it the largest and the most homogeneous sample of RR Lyrae stars in the given stellar system. More than 27 000 are of RRab type, up to 11 000 are of RRc stars, and almost 200 are double-mode variables of RRd type. This is a significant increase in detection of RR Lyrae stars. For a comparison, in OGLE-III ([Soszyński et al., 2011](#)) only about 16 000 RR Lyrae stars were detected.

The coverage of the Galactic bulge is shown in Fig. 4.1. Dodecahedra show the field of view of the CCD camera. Coloured fields denote well-covered areas of the Galactic bulge. The most observed fields are marked with a red colour. A number of photometric observations varied from several hundreds up to several thousands. The classification of a single star as an RR Lyrae star

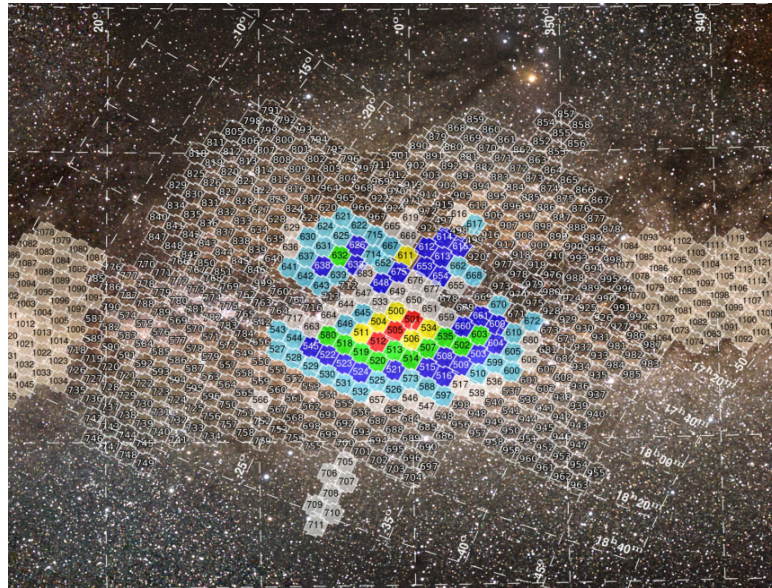


Figure 4.1: Observed fields in the Galactic bulge in OGLE-IV survey, coloured sections indicate well observed fields. Red fields are the most observed fields with more than 8000 observations per star (taken and modified from [Udalski et al. \(2015\)](#)).

was based on two methods. First, for stars with the periods in the interval $\langle 0.2; 1.0 \rangle$ days, Fourier coefficients were determined and then compared with Fourier parameters of typical RR Lyrae stars. The second method consisted of creating template light curves of RRab and RRc stars, and then compared with the observed data. Overall, the final visual inspection of the light curves was

pivotal. The general completeness of all RR Lyrae stars in the Galactic bulge is close to 95 %, integrity, of course, slightly differs for each type (Soszyński et al., 2014).

4.2 Sample selection

In this thesis, we look for the Blazhko effect among RRab type of stars in the *I*-band photometry of OGLE-IV survey. From the entire sample of 27 258 RRab stars in OGLE-IV, not all of them were suitable for search of the Blazhko modulation. To ensure homogeneity and reliability of our analysis we set up following criteria:

1. Stars below the Galactic latitude $b = -8^\circ$ were removed, due to their possible affiliation to the Sagittarius tidal stream and not to the Galactic bulge.
2. Objects with mean *I*-band magnitude above 18 mag were removed due to a large scatter.
3. Stars from globular clusters were dismissed.
4. Stars from *remarks.txt*¹ were removed. This file contains a list of stars with unclear affiliation to RR Lyraes subtypes.
5. Only *I*-band photometry was used, and after a visual inspection we decided to use only stars with more than 425 points.
6. Stars identified as possible RR Lyrae stars in binaries were also removed Hajdu et al. (2015).

For a map of the Galactic bulge with analysed stars see Sect. 5.1, where we discuss spatial distribution of Blazhko stars. In the end, the remaining sample consisted of 8 283 stars with a number of observations for selected stars ranging from 425 to 8 300 points. The median value of a number of measurements was above 1 060 points per star. The Fig. 4.2 shows two histograms. The one on the left displays complete distribution of observations per star. We can notice six major groups with approximately 500, 1000, 3000, 5500, 6000 and 8000 points. This distribution corresponds to the map for observed fields in the Galactic bulge (Fig. 4.1). The right panel in Fig. 4.2, shows distribution of mean magnitude in *I*-band. The median lies at 16.368 mag. In addition, unlike for faint stars, we did not remove any bright stars. Therefore, few individual stars might actually lie in front of the Galactic bulge.

¹<ftp://ftp.astrouw.edu.pl/ogle/ogle4/OCVS/blg/rrlyr/>

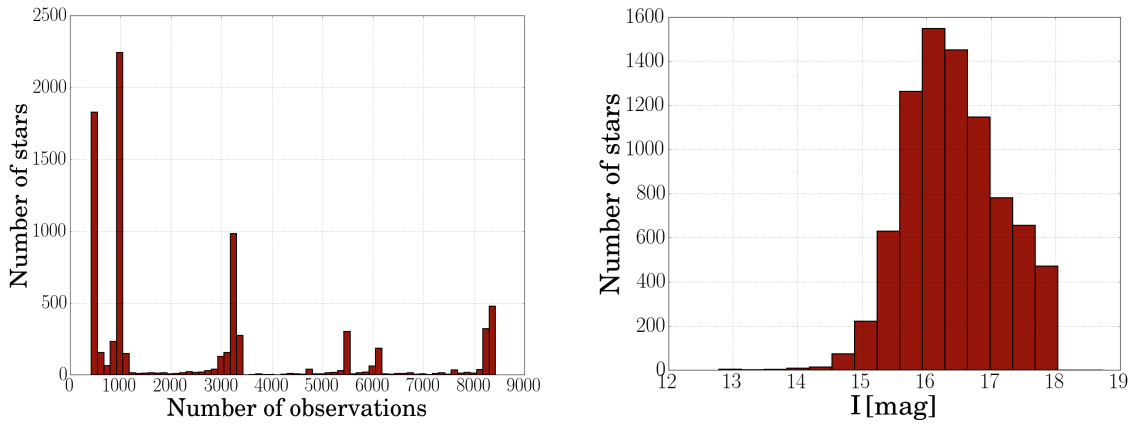


Figure 4.2: Distribution of the number of measurements per star and distribution of mean magnitude for stars in our sample. In the left-hand panel we see six peaks for number of observations per stars that well correspond dodecahedra in Fig. 4.1. The right-hand panel shows a histogram for mean brightness in I -band of selected stars. Data from OGLE-IV, [Soszyński et al. \(2014\)](#).

The mean photometric error of a single point for stars with mean $I < 15.5$ mag is 0.004 mag, and for faint stars with mean $I < 17.8$ mag it is 0.02 mag. The TS for each RR Lyrae star in OGLE-IV ranged between 1300 and 1400 days. Together with photometric data, a complete catalogue with light elements, mean brightness, peak-to-peak amplitudes and Fourier parameters was published by [Soszyński et al. \(2014\)](#). These values will be further used in this thesis.

The phase and raw light curve of each star (example in Fig. 4.3) was then visually inspected, and each star was assigned to one of the three categories – clear Blazhko effect, candidate, no modulation apparent. This procedure was purely subjective, but helped identify interesting cases and stars with significant outliers.

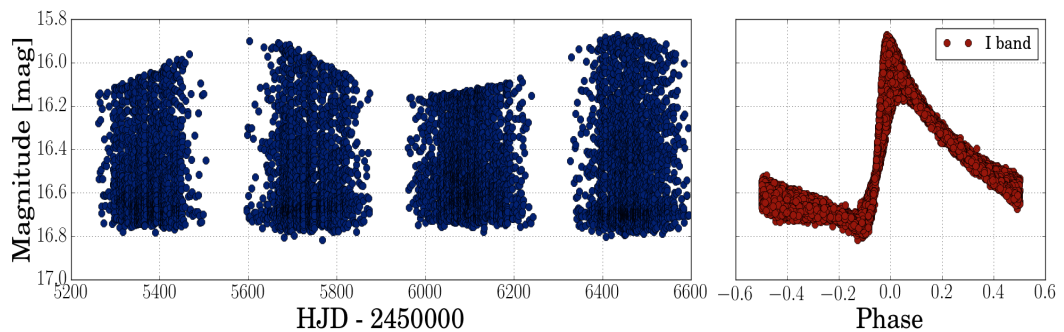


Figure 4.3: Example of time distribution of the data (left-hand panel) and data phase with pulsation period (right-hand panel) shown on OGLE-BLG-RRLYR-07296. Figures like these served for visual identification of stars with the Blazhko effect. Data from OGLE-IV, ([Soszyński et al., 2014](#)).

4.3 Semi-automatic analysis

The Blazhko effect exhibits itself in a frequency spectrum as equidistant peaks in close vicinity of the basic pulsation frequency and its harmonics (see Sect. 3.1). Thus, we searched for side peaks from the frequency spectrum, because side peaks usually have smaller amplitudes than kf_0 .

The strategy of the analysis proceeds from the methods used by Skarka (2014a). For a complete period analysis we can use PERIOD04 (Lenz & Breger, 2004). However, the period analysis and consecutive prewhitening with found frequencies using PERIOD04 is extremely time-consuming. For instance, it can take from a couple of minutes up to several hours, to gain full light curve solution for a star from OGLE-IV survey.

For an unmodulated star with approximately 1 000 measurements with mean brightness around 17 mag we found in the frequency spectrum around 8 harmonics of f_0 . For unmodulated, brighter and more observed stars, the number of detectable harmonics could rise up to $30 f_0$. Therefore, we decided to employ a semi-automatic approach for the search of the Blazhko modulation.

For each star, we applied NLLSM (Levenberg–Marquardt algorithm) using trigonometric polynomial to remove the main pulsation frequency and kf_0 harmonics (where $k = 2, 3, \dots, 10$), instead of doing it manually. Residuals, gained from this prewhitening, were analysed using PERIOD04. To ensure coherent analysis, we created a test sample of one hundred stars. Each star from the test sample was analysed manually using PERIOD04, and semi-automatically using NLLSM followed by the analysis of residuals in PERIOD04. Results from both approaches were the same allowing us to apply the semi-automatic approach to the entire data sample.

The analysis proceeded in two basic steps. First, we used NLLS prewhitening to create residual file. Using PERIOD04 we analysed these residuals while searching for the Blazhko modulation in the close neighbourhood of the removed main pulsation frequency and the first harmonic. We did not look for the Blazhko frequency itself, due to reasons described in Sect. 3.1. To consider a star as a Blazhko star, several conditions had to be fulfilled. First, in the frequency spectrum we had to find at least two equidistant peaks for Blazhko modulation. Both of these peaks had to have signal to noise ratio (S/N) larger than 3.5 to be considered as real. Stars with the Blazhko modulation longer than $TS/2$ were analysed using OGLE-III data with fewer points and lower quality than OGLE-IV, but longer TS (up to 4 500 days). This allowed us to confirm or deny some of the long Blazhko periods.

Due to the fact that we did not remove any outliers, the NLLS fit did not work correctly for stars with low number of points and strongly distorted light curves (strong Blazhko modulation). Therefore, these stars were processed manually. Several dozens of stars that were visually (based on a shape of light and phase curve) identified as the Blazhko stars did not show any modulation in the frequency spectrum. These stars were also manually analysed to ensure correct results. Several dozens of these anticipated modulated stars exhibited so far undocumented additional periodicities (see Sect. 6.2).

Someone might argue, why a fully automatic procedure was not used. This approach would be faster but we must not forget how complicated the frequency spectra of RR Lyrae stars are. The OGLE-IV is a ground-based survey, thus, we can expect numerous aliases and false peaks. In addition, we would probably miss interesting cases of Blazhko modulation and perhaps even some Blazhko stars (Skarka, 2014a). Furthermore, stars with additional periodicities (see Sect. 6.2) would be probably missed. Therefore, using the semi-automatic approach we still have supervision over the period analysis, while exploiting opportunities to accelerate the process. After adjusting of all procedures, the analysis of a single star did not exceed 10 minutes.

Because the main goal was to identify stars with modulation, we did not deal with any additional details of the frequency spectra suggesting e.g. multiple Blazhko effect and variations of the Blazhko effect itself. We just made a comment. In addition, we did not write down amplitudes of modulation peaks. Detailed analysis of these stars is out of scope of this thesis. Thorough analysis of modulation properties will be targeted in forthcoming study.

Chapter 5

Results

THE main goal of presented thesis is to identify RR Lyrae stars with the Blazhko modulation in the Galactic bulge using OGLE-IV data. Such identification allowed us to determine the incidence rate of the Blazhko stars in the Galactic bulge and investigate the differences between modulated and unmodulated stars on the basis of their light curves. In addition, a relation between pulsation and modulation period could be found. In this analysis, we examined one of the largest and the most homogeneous samples of RR Lyrae stars ever studied regarding the Blazhko effect.

So far, only three papers dealing with RR Lyraes in the Galactic bulge using OGLE survey were published (Mizerski, 2003; Collinge et al., 2006; Soszyński et al., 2011). Mizerski (2003) and Collinge et al. (2006) used data from OGLE-II, and Soszyński et al. (2011) used data from OGLE-III. Of the aforementioned authors only Collinge et al. (2006) provided a list of stars with the Blazhko effect. Therefore, we can compare our findings with their results.

5.1 Fraction of Blazhko stars

From our entire sample of 8 283 RRab type stars, 38 % stars exhibited the Blazhko modulation, 4 % stars were marked as possible candidates and 58 % stars did not show any sign of modulation (see tab. 5.1). For comparison, Alcock et al. (2003) found 12 % (731 stars) Blazhko stars in the LMC, 28 % (526 stars) modulated stars were reported by Collinge et al. (2006) in the Galactic bulge, 355 Blazhko stars are known in the Galactic field (actual online version of BlaSGalF database, Skarka, 2013).

In comparison with the previous studies on the Galactic bulge, 38 % is a high incidence rate. Mizerski (2003) found 25 % stars to be modulated, Collinge et al. (2006) reported 28 %, and Soszyński et al. (2011) discovered 30 % of RRab type stars exhibiting the Blazhko effect. There could be several reasons for higher percentage of the Blazhko effect detected by us. First, data quality and coverage of OGLE-IV photometry is significantly better. Second, in the papers by Mizerski (2003), Collinge et al. (2006) and Soszyński et al. (2011) automatic routines were used to determine the Blazhko modulation.

Third, in contrast with their studies, we did not use the entire sample of RRab stars from OGLE-IV survey. We used only the most well-observed stars, to reduce the probability of missing a star with the Blazhko effect. From above-mentioned authors, only Collinge et al. (2006) provided a list of 526 modulated stars, from which we analysed, due to our criteria, 418 stars. Interestingly, 6 of these stars did not show any sign of modulation, 6 stars were marked as candidates, and in the rest of the stars we achieve conformity with our analysis.

Our study presents larger ratio of modulated/unmodulated stars and is in better agreement with the latest studies of occurrence of the Blazhko effect (see Sect. 3.1). However, it does not reach 50 % as the studies by Jurcsik et al. (2014) and Benkő et al. (2011). This could simply be their observation bias, because Benkő et al. (2011) and Jurcsik et al. (2014) analysed only couple dozens of RR Lyraes stars. On the other hand, it could be a real attribute of the Galactic bulge. In *Kepler* K2 campaigns 9 and 11, the focus will be at the Galactic bulge, and over 2 000 RR Lyrae stars will be observed. Perhaps, the forthcoming *Kepler* campaigns will shed new light on the Galactic bulge RR Lyraes and give more confident estimations of the fraction of modulated stars. Table 5.1 presents exact numbers of stars for given category.

Table 5.1: Table with numbers and percentage ratios of modulated and unmodulated stars.

	# number of stars	% percentage
Unmodulated stars	4 785	58 %
Stars with the Blazhko effect	3 168	38 %
Candidates	330	4 %

Regarding the stars that fell into the candidate category, they can be divided into two groups. The first group showed only one peak for possible Blazhko modulation, therefore, we cannot conclusively say that these stars have the Blazhko modulation (approximately 30 % of the candidates). The second group displayed additional peaks in the frequency spectrum that could be interpreted as the Blazhko modulation. Unfortunately, periods of the possible Blazhko modulation for stars from the second group exceeded the criterion for the length of Blazhko period ($P_{BL} > TS/2$). These stars can actually undergo period change, that can somewhat mimic the Blazhko effect in the frequency spectrum. To determine whether stars from the second candidate group undergo a period change or exhibit the Blazhko effect, we used data from OGLE-III survey. Unfortunately, not all stars from our sample have data in OGLE-III¹, therefore, they stayed in the candidate category. Some stars that actually had data in OGLE-III exhibited too long modulation periods that even the data from OGLE-III was not long enough to decide about modulation. For

¹The OGLE-III survey consists of only 11 756 RRab stars while OGLE-IV of 27 258 RRab stars.

these stars, we decided to keep them in the candidate category, to preserve the integrity of our sample.

In Fig. 5.1, we see a map of the Galactic bulge consisting only of stars that were analysed in this study. The blue dots represent stars without the Blazhko effect, while red dots stand for stars with modulation. Comparing Figs. 5.1 and 4.1, we can notice that our selection comprises stars exclusively from coloured fields, that is with the most numerous data. It is apparent that only stars from the inner bulge were analysed. We searched for overdensities of modulated or unmodulated stars. So far we were unable to find any inhomogeneous region with significantly larger, or lower population of stars with the Blazhko modulation. We note, that for proper analysis of overdensities in the Galactic bulge we would need distances for individual stars. This analysis will be objective in our future study.

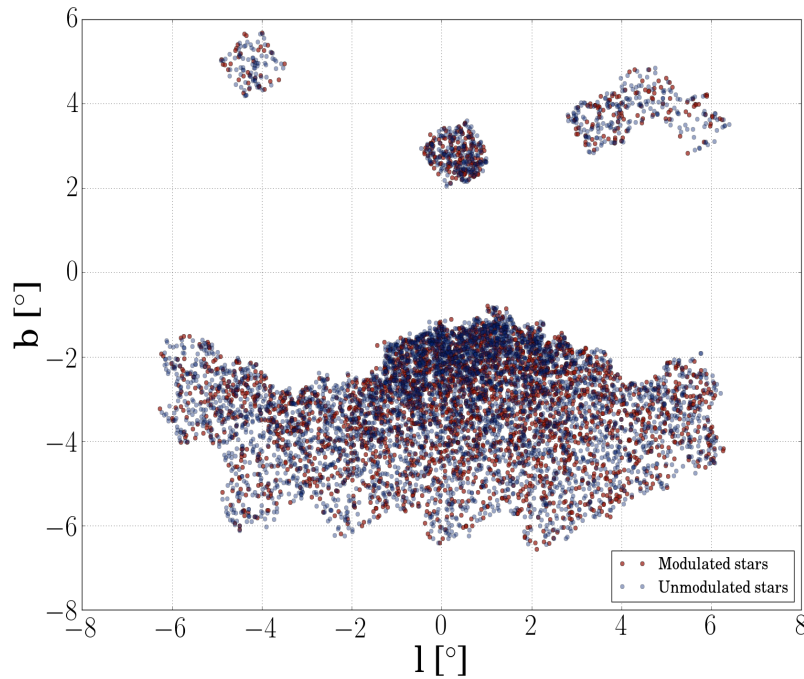


Figure 5.1: A map of the Galactic bulge with blue dots representing stars with the Blazhko effect and red dots representing stars without the Blazhko modulation.

5.2 Period distribution

In Sect. 3.4 we stated that one of the differences between modulated and unmodulated stars could be in their pulsation periods. Our results seem to support this claim. In Fig. 5.2 we see a histogram of pulsation periods for Blazhko stars (red columns) and unmodulated stars (blue columns). In this distribution, we see that Blazhko stars have almost normal distribution while

unmodulated stars have non-Gaussian distribution. From this figure, we see a small shift to lower periods for modulated stars. The average of pulsation periods for Blazhko stars is 0.53(6) days while for non-Blazhko counterparts is 0.56(9) days. The median of pulsation periods for modulated and unmodulated stars are fairly similar to averages, 0.530 and 0.558 respectively. The similar results for modulated stars were derived by [Skarka et al. \(2016\)](#). They propose that all known modulated stars have the Gaussian distribution of pulsation periods with a midpoint at 0.54(7) days.

The difference between modulated and unmodulated stars in pulsation periods can be affected by non-Gaussian distribution of pulsation periods. In addition our results for modulated and unmodulated stars are within errors the same, therefore the difference could be considered as insignificant.

The fraction of the Blazhko effect for long pulsation periods significantly declines. For periods longer than 0.65 days, the incidence rate of the Blazhko effect drops to 14%. Among stars with pulsation periods shorter than 0.65 days, the percentage of modulated stars is 42%. The percentage of stars with the Blazhko effect, for some short pulsation periods, rose almost to 50%, contrary to long pulsation periods, where for some intervals we were unable to find any star with the Blazhko effect at all.

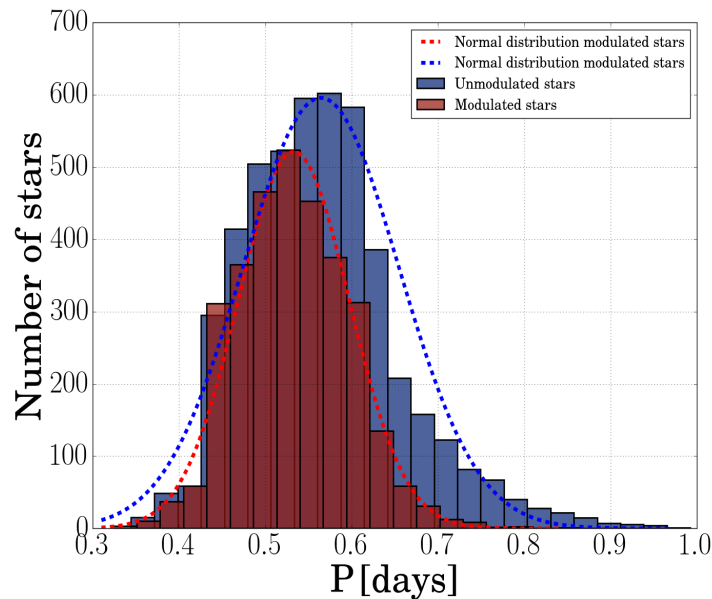


Figure 5.2: Distribution of pulsation periods for stars with the Blazhko effect (red columns) and for unmodulated stars (blue columns). For comparison, we added model of normal distribution (dashed lines) for both groups.

The star with the Blazhko effect with the longest pulsation period is OGLE-BLG-RRLYR-11213. This star has a pulsation period $P = 0.84326111(30)$ days, and the period of the Blazhko modulation of $P_{BL} = 29.03(5)$ days. On the opposite side lies OGLE-BLG-RRLYR-09012 with $P = 0.32399241(27)$ days, with the Blazhko modulation period $P_{BL} = 37.72(3)$ days. The errors for modulation

periods were gained from least-square method. An example of a complete list of Blazhko stars with modulation periods is in table 5.2.

Table 5.2: A table for stars with the Blazhko effect. For complete listing, with additional information, see <http://physics.muni.cz/~prudil/Blazhko-stars/Blazhko-stars.txt>.

# Name	P_{BL} [days]	err P_{BL} [days]	...
OGLE-BLG-RRLYR-00162	172	1	...
OGLE-BLG-RRLYR-00172	118.8	0.7	...
⋮	⋮	⋮	...

Periods for the Blazhko modulation span from 4.85 days up to 2 198 days, with the median at 60.45 days. The star with the longest Blazhko period, OGLE-BLG-RRLYR-06232, is probably the outermost boundary for OGLE-III and OGLE-IV data. The OGLE-BLG-RRLYR-08834 with $P_{BL} = 4.85(34)$ days is a star with the shortest known Blazhko period. In addition, it is the first star with Blazhko period below 5 days. The Fig. 5.3 shows a histogram for modulation periods and plot with cumulative distribution function. Distribution of Blazhko periods follows log-normal distribution with average at 1.85(42) dex. Similar result was obtained by Skarka et al. (2016). Their log-normal distribution of Blazhko periods have midpoint at 1.78(30) dex.

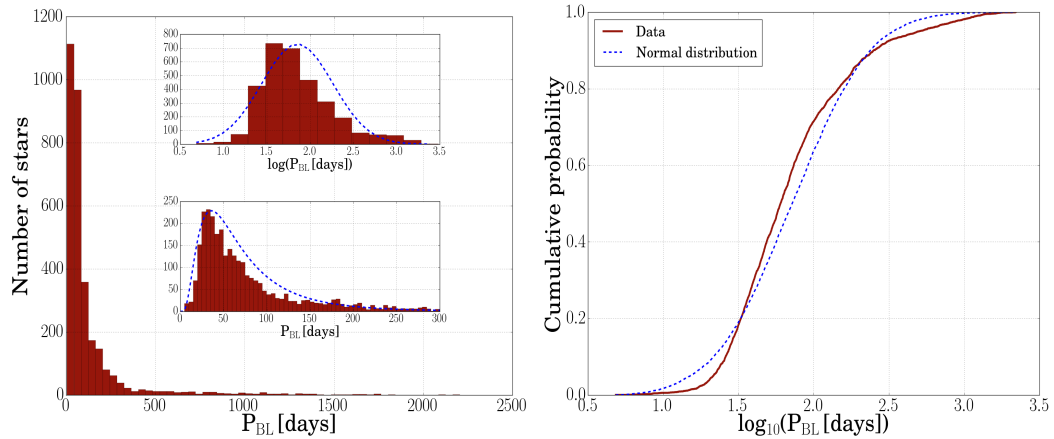


Figure 5.3: This figures show distribution of modulation periods (left-hand panel) and cumulative distribution function (right-hand panel). The left-hand panel shows a histogram of modulation periods for stars with the Blazhko effect (red columns) and fit for normal distribution (blue dashed line). The right-hand panel displays cumulative distribution function for identified Blazhko stars.

Another interesting comparison is for modulation and pulsation frequency. The relation connecting these two parameters (in eq. 3.8) had been reported for the upper limit by Jurcsik et al. (2005). The Fig. 5.4 shows our analysed sample of RR Lyraes with the Blazhko effect, and a figure taken from Jurcsik et al. (2005). Unlike Jurcsik, we did not use data for the first-overtone pulsators. In our figure we see a clump of points at the bottom of the plot.

Despite few points somewhat following [Jurcsik et al. \(2005\)](#) relation, we cannot conclusively confirm their findings. This discrepancy is probably caused by not including RRc stars.

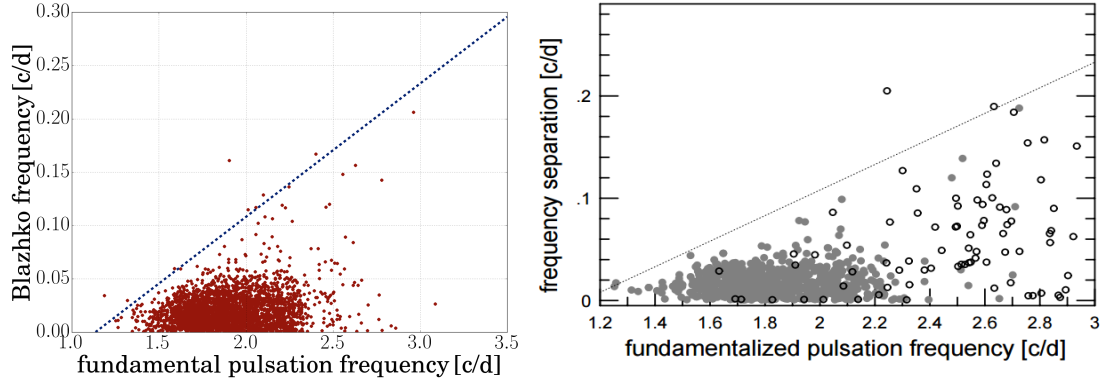


Figure 5.4: Blazhko frequency as a function of the pulsation frequency. The left-hand panel shows data from our study (red dots) and blue line is based on relation 3.8. The right-hand panel shows for comparison plot from [Jurcsik et al. \(2005\)](#). Filled points represents RRab stars while empty RRc stars with fundamentalized pulsation frequency.

In Fig. 5.5 we see two density diagrams for logarithm of modulation periods as a function of pulsation periods. The left-hand panel shows data for the Galactic bulge and we see a large group between $\log_{10}(P_{BL}) = 1.5 - 2.0$. The right-hand panel displays similar density diagram, but with 1550 stars collected from the literature from the Galactic bulge, LMC, M5, and the Galactic field ([Skarka et al., 2016](#)). The agreement between the plots is very good suggesting that the Blazhko periods have identical distribution in all mentioned systems.

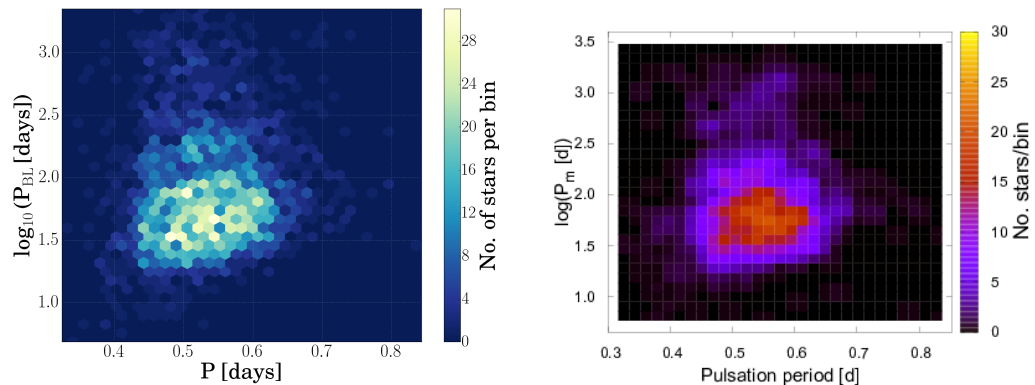


Figure 5.5: Density diagrams for pulsation vs. modulation periods. The left-hand density diagram shows our analysed sample of RR Lyraes exhibiting the Blazhko effect. The right-hand panel shows similar density for stars from the Galactic field, the LMC, the Galactic bulge and stars from M5, ([Skarka et al., 2016](#)).

In Fig. 5.5 nor in Fig. 5.4 we do not see any relation between pulsation and modulation periods in our data. Therefore, there is most likely no connection between pulsation and Blazhko periods in RRab stars.

5.3 Amplitude distribution

One of the known differences between stars with the Blazhko effect and stars without modulation is in total amplitudes. In Fig. 5.6 we see three panels. The top panel shows a distribution of pulsation periods based on stars affiliation to modulated or unmodulated group. The bottom left panel is Bailey's diagram (see Sect. 1.1) for RRab stars from our sample, with red dots representing modulated stars and blue dots unmodulated stars. In this subplot, we can clearly see the OoI and some stars with long periods that can belong to the OoII. The vast majority of stars in our sample belong to the OoI. However, Pietrukowicz et al. (2015) in their paper reported the presence of multiple old populations in the Galactic bulge. These two populations within the OoI are most likely the results of merges from the early evolution of the Milky Way. The bottom right panel shows the histogram for the amplitude distribution of modulated/unmodulated stars. We noticed a difference in occurrence of the Blazhko effect for different amplitudes.

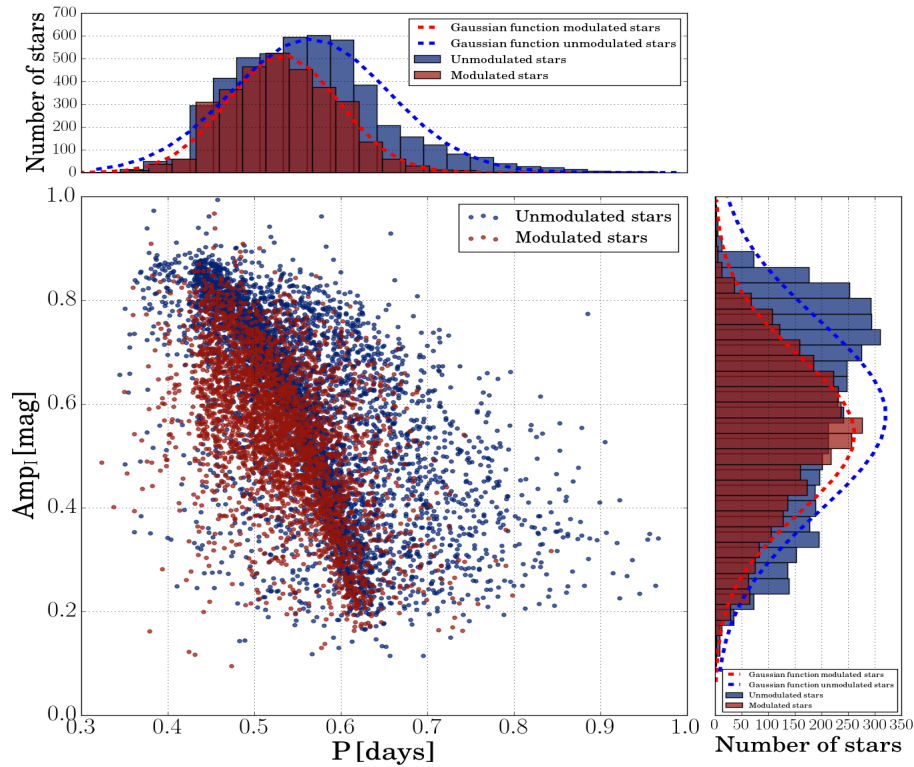


Figure 5.6: Figure showing distribution of the pulsation periods and amplitudes. The bottom left figure is a period-amplitude diagram consisting of two groups of stars, modulated (red dots) and unmodulated (blue dots). Top panel shows a histogram for pulsation periods with the Gaussian fit (for values of midpoints see Sect. 5.2). The panel on the right is the distribution of total amplitudes with the Gaussian fit.

For amplitudes that belong to the interval $\langle 0.48; 0.62 \rangle$ mag, the incidence rate of the Blazhko effect reaches, and in some cases even exceeds, 50 %, whereas,

for shorter periods and higher amplitudes, outside this interval, the fraction drops to 30 %, or even less. The amplitudes of unmodulated stars show strong non-Gaussian distribution with possible two populations, while modulated stars show almost the quite opposite. This is probably caused by higher percentage of modulated stars around medium values of amplitudes. When we consider all stars from our sample as one group, then the distribution is Gaussian. Midpoint amplitudes of modulated stars lie at $\mu_{\text{BL}} = 0.54(15)$ mag, and for unmodulated $\mu_{\text{NONBL}} = 0.58(19)$ mag. Due to a non-Gaussian distribution for unmodulated stars, the uncertainties could be skewed.

The difference in total amplitudes for modulated and unmodulated stars is seen in Fig. 5.7. For this plot, we first divided our sample into thirty bins based on pulsation periods. Then we calculated the difference in median amplitudes for unmodulated and modulated stars (vertical axis $\Delta \text{Amp}_I = \text{Amp}_{I-\text{median}}^{\text{NONBL}} - \text{Amp}_{I-\text{median}}^{\text{BL}}$). We note that Fig. 5.7 does not show the whole period spectrum. The groups with pulsation periods longer than 0.7 days and shorter than 0.37 days were removed due to a low number of modulated stars. Dispersion in short periods (from 0.370 to 0.425 days) and long periods (from 0.625 to 0.685 days), is most likely caused by a lack of stars in both groups (for the short periods we had only 20 – 55 stars per group). For long periods, despite a large amount of stars (from 77 to 233), we did not have a sufficient number of Blazhko stars (only a couple of dozens). For a comparison, in groups with periods around 0.5 days, we had almost 500 stars with ratio modulated/unmodulated stars around 50 %. In overall, our results, despite the dispersion, suggest that modulated stars have smaller amplitudes than unmodulated counterparts by a factor of 0.028(45) mag. This values support [Alcock et al. \(2003\)](#) and [Szeidl \(1988\)](#) findings, giving this difference explicit value.

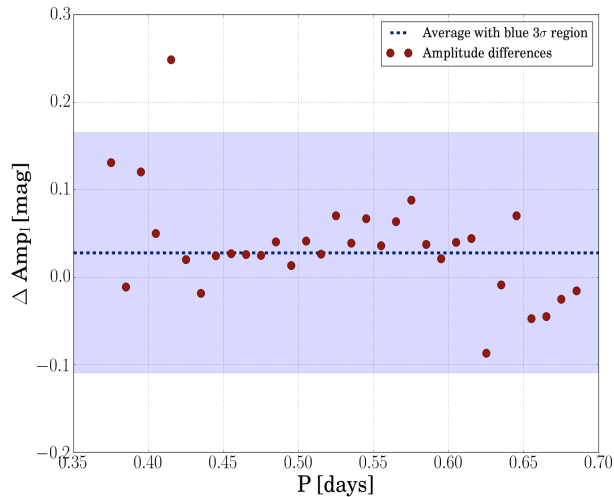


Figure 5.7: Plot with groups of stars divided on the basis of their pulsation periods. The vertical axis represents differences between median values of amplitudes of unmodulated and modulated stars in thirty bins. The horizontal line outlines the average difference in amplitudes with 3σ filled region.

In Fig. 5.8 we see two density diagrams with model describing the OoI population in the Galactic bulge (see Sect. 6.1). The left-hand figure represents period-amplitude diagram for unmodulated stars, while figure on the right shows the same dependence but for modulated stars. The vast majority of unmodulated stars seems to follow the OoI and extend to longer periods. The Blazhko stars do the quite opposite, they evade long pulsation periods and seem to fall below the OoI. The Fig. 5.8 nicely shows the difference in amplitudes between modulated and unmodulated stars.

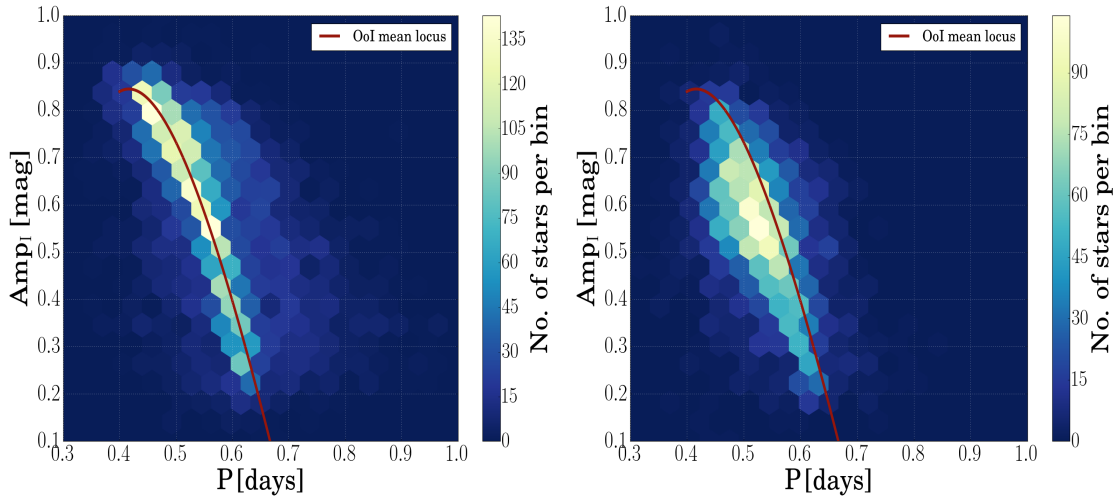


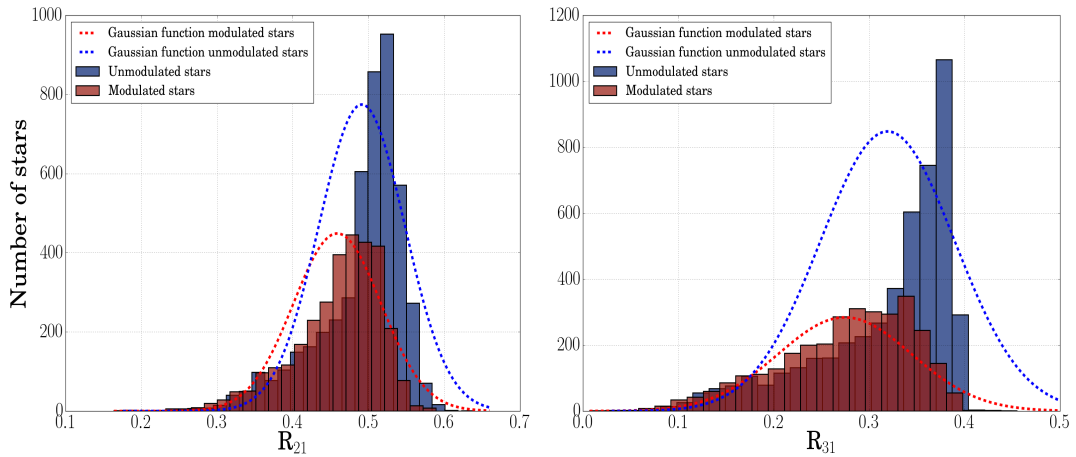
Figure 5.8: The distribution of amplitudes and pulsation periods. The left-hand density diagram shows the number of stars for given amplitude and pulsation period. The right-hand diagram shows, the density plot for modulated stars. Red line in both plots represents a model of the OoI in the Galactic bulge, for detailed description see Sect. 6.1.

5.4 Fourier coefficients R_{21} and R_{31}

Fourier parameters R_{21} and R_{31} , gained from the trigonometric fit are connected with amplitudes through relation 2.28. Because there are differences in total amplitudes, we can expect to see some differences between modulated and unmodulated stars also in R_{ij} . The plots in Fig. 5.9 show a distribution of stars for given Fourier coefficients. In both plots, we can notice, that incidence rate of Blazhko stars differs. For lower values of R_{21} and R_{31} the fraction of the Blazhko effect rises to 50% and sometimes even to higher values. On the other hand, for higher values of Fourier coefficients, the rate of Blazhko stars quickly drops. In addition, neither of these coefficients seem to follow the normal distribution. The average values of the Gaussian distribution $\mu^{R_{ij}}$, for individual coefficients can be found in table 5.3. We see that approximate mid-points for Gaussian distribution differ for modulated and unmodulated stars. Difference for R_{21} is 0.03, and for R_{31} it is 0.05.

Table 5.3: The average and median values for given Fourier parameters R_{21} and R_{31} .

Average	
$\mu_{\text{BL}}^{R_{21}} = 0.46(6)$	$\mu_{\text{BL}}^{R_{31}} = 0.27(7)$
$\mu_{\text{NONBL}}^{R_{21}} = 0.49(6)$	$\mu_{\text{NONBL}}^{R_{31}} = 0.32(7)$
Median	
$\mu_{\text{BL}}^{R_{21}} = 0.47$	$\mu_{\text{BL}}^{R_{31}} = 0.29$
$\mu_{\text{NONBL}}^{R_{21}} = 0.51$	$\mu_{\text{NONBL}}^{R_{31}} = 0.35$

**Figure 5.9:** The distribution of modulated and unmodulated stars for Fourier coefficients R_{21} and R_{31} . The left-hand panel represent histograms for R_{21} with modulated stars (red columns) and unmodulated stars (blue columns). The right-hand panel depicts similar histogram for R_{31} with modulated stars (red columns) and unmodulated stars (blue columns). In addition, they both contain interpolations for the normal distribution.

The Fig. 5.10 shows pulsation period– R_{21} and pulsation period– R_{31} dependence, respectively. The left-hand plots show only stars without modulation, while the right-hand panels show both groups combined. The Blazhko stars clearly occupy mainly the region with shorter periods and lower values of R_{21} and R_{31} . This can be also seen in Figs. 5.9 and 5.2. Quantitatively speaking, for $R_{21} > 0.525$ (approximately 1 600 stars), the incidence rate of the Blazhko effect drops to 14 %. For coefficient R_{31} , the incidence rate is 15 % for a limit of 0.35 (approximately 2 600 stars). Analogous results were reported by Skarka (2014b). He likewise reported a decrease in the incidence of the Blazhko effect for higher values of R_{21} and R_{31} .

In the left-hand plots of Fig. 5.10, we can notice several populations of RR Lyrae stars. The first two are probably the OoI and the OoII stars. The OoI extends in a well covered stream down at the period of 0.625 days. The situation with the OoII is rather complicated because we do not see downward stream as in the OoI. We see an arm propagating to longer periods. To better

describe the OoII we would need more stars. In addition, in the OoI descending stream (to lower values of R_{21} and R_{31}) we can notice a barely apparent duality of this branch. This might be Population A and Population B mentioned by Pietrukowicz et al. (2015).

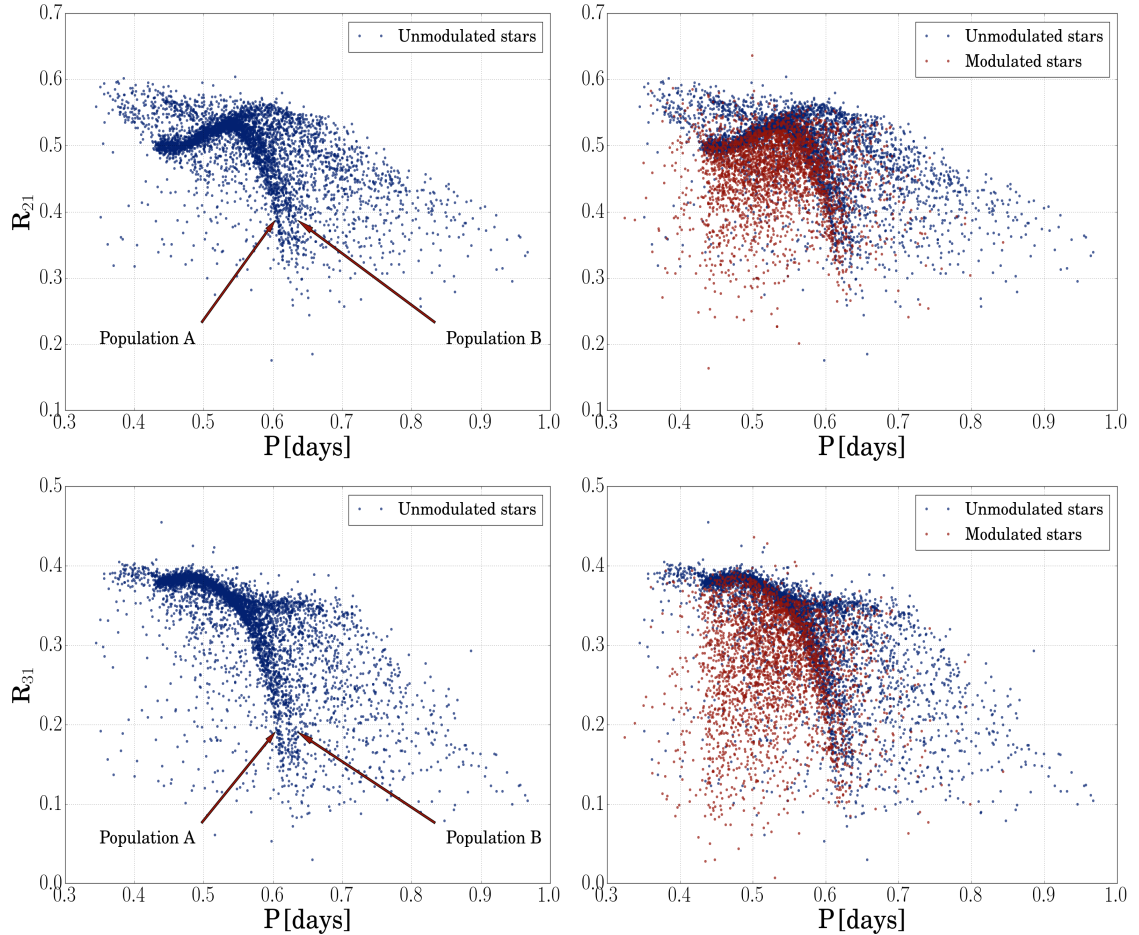


Figure 5.10: Fourier amplitude ratios versus pulsation periods of stars from our sample. The left-hand figures show pulsation period– R_{21} and pulsation period– R_{31} dependences only for unmodulated stars, while the plots on the right-hand include modulated and unmodulated stars.

5.5 Fourier coefficients φ_{21} and φ_{31}

Fourier parameters φ_{21} and φ_{31} play the key role when determining physical parameters of RR Lyrae stars. They are derived using relation 2.29.

The Fig. 5.11 shows histograms for the phase coefficients. In both plots, we can notice that the incidence rate of the Blazhko effect differs for various parameters. For lower values of φ_{21} and φ_{31} the probability of finding the Blazhko effect rises while for higher values decreases. As in previous Sect. 5.4, neither φ_{21} nor φ_{31} seem to follow the Gaussian distribution. The reason for this could be a presence of two Oosterhoff populations. In table 5.4

we can find the average and median for given Fourier coefficients and modulated/unmodulated stars. The difference between modulated and unmodulated φ_{21} is 0.09 rad while for φ_{31} it is 0.22 rad. The differences in midpoints for both phase parameters are mild, but very well visible in both histograms of Fig. 5.11.

Table 5.4: The average and median values for given Fourier parameters φ_{21} and φ_{31} .

Average	
$\mu_{\text{BL}}^{\varphi_{21}} = 4.36(22) \text{ rad}$	$\mu_{\text{BL}}^{\varphi_{31}} = 2.61(47) \text{ rad}$
$\mu_{\text{NONBL}}^{\varphi_{21}} = 4.45(26) \text{ rad}$	$\mu_{\text{NONBL}}^{\varphi_{31}} = 2.83(50) \text{ rad}$
Median	
$\mu_{\text{BL}}^{\varphi_{21}} = 4.33 \text{ rad}$	$\mu_{\text{BL}}^{\varphi_{31}} = 2.55 \text{ rad}$
$\mu_{\text{NONBL}}^{\varphi_{21}} = 4.44 \text{ rad}$	$\mu_{\text{NONBL}}^{\varphi_{31}} = 2.79 \text{ rad}$

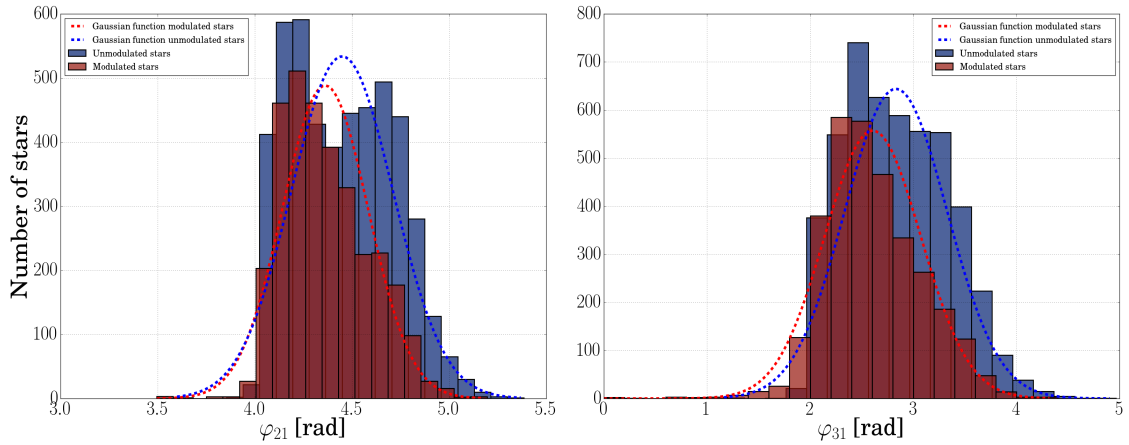


Figure 5.11: Both plots displays distribution of modulated and unmodulated stars for Fourier coefficients φ_{21} and φ_{31} . Histograms for φ_{21} (left-hand panel) and φ_{31} (right-hand panel). The stars are divided into two groups according to a presence of modulation. Plots are interpolated with Gaussian function.

The coefficient φ_{31} is with pulsation period used in numerous relation to calculate metallicity of RR Lyrae stars. For *I*-band, Smolec (2005) derived a relation based on OGLE survey

$$[\text{Fe}/\text{H}] = -3.142 - 4.902P + 0.824\varphi_{31} \quad , \quad \sigma = 0.18 \quad (5.1)$$

Results for calculated metallicity in modulated and unmodulated stars are in Fig. 5.12. We note that Fourier parameters in OGLE-IV survey were determined using cosine trigonometric polynomial, not sine as in 2.23. The relation

for metallicity 5.1 is calibrated to sine, therefore we had to transform φ_{31} coefficient to sine. We used simple formula

$$\varphi_{31}^{\sin} = \varphi_{31}^{\cos} - \pi . \quad (5.2)$$

Considering differences in φ_{31} and in pulsation periods between unmodulated stars and Blazhko stars, one would expect to see a difference also in metallicity. But we did not find any difference at all. The ratio of Blazhko stars is slightly higher for lower metallicities, but considering differences in other parameters, the variation in metallicity between modulated/unmodulated stars is very mild. Therefore, it is safe to say, that the Blazhko effect has almost no connection to metallicity in the Galactic bulge. The average value for modulated stars is $-1.02(26)$ dex and for unmodulated is $-0.98(30)$ dex. Therefore, photometric metallicities of modulated stars and unmodulated stars could be considered as identical.

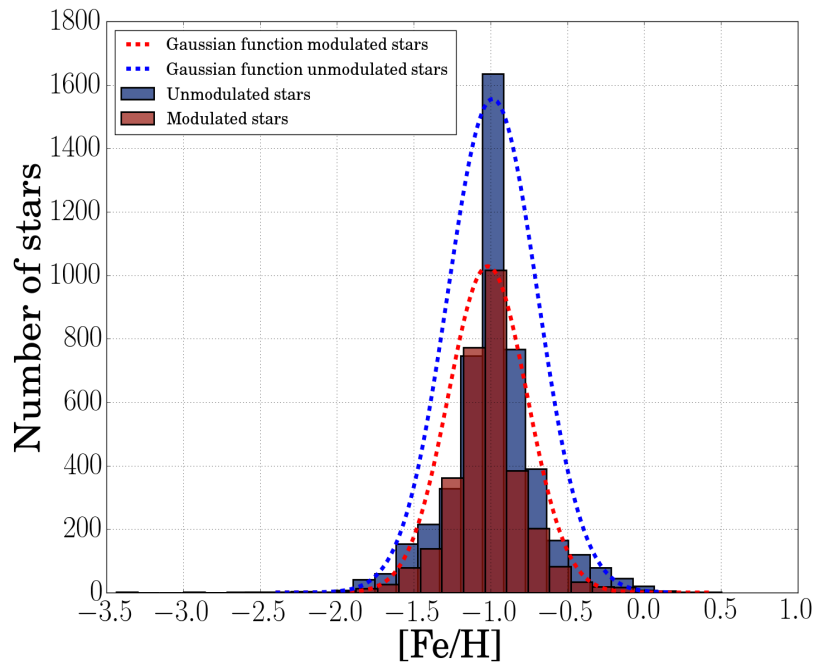


Figure 5.12: Distribution of metallicity for stars with the Blazhko effect (red columns) and for unmodulated stars (blue columns). In addition, model of Gaussian function is included for both groups.

The Fig. 5.13 illustrates dependence of R_{31} on phase parameters φ_{21} and φ_{31} . The graphs on the left show only unmodulated stars while plots on the right include both, modulated and unmodulated stars. The figures for unmodulated stars show two populations of RR Lyrae stars in the Galactic bulge (double-hook shape structures). These two groups probably belong to the OoI and the OoII populations. When we include Blazhko stars (the right-hand plots) we see a very distinctive difference between modulated and unmodulated stars.

While stable stars seem to clearly follow the hook shape trend, modulated stars, in addition, populate area below this dependence. For values of φ_{21} below 4.5 rad and values of R_{31} below 0.3, the percentage of the Blazhko effect rises above 97 %. From a total of 1 187 stars in this region, only couple dozens of stars showed no sign of modulation. These stars were manually analysed to assure that they are indeed without modulation.

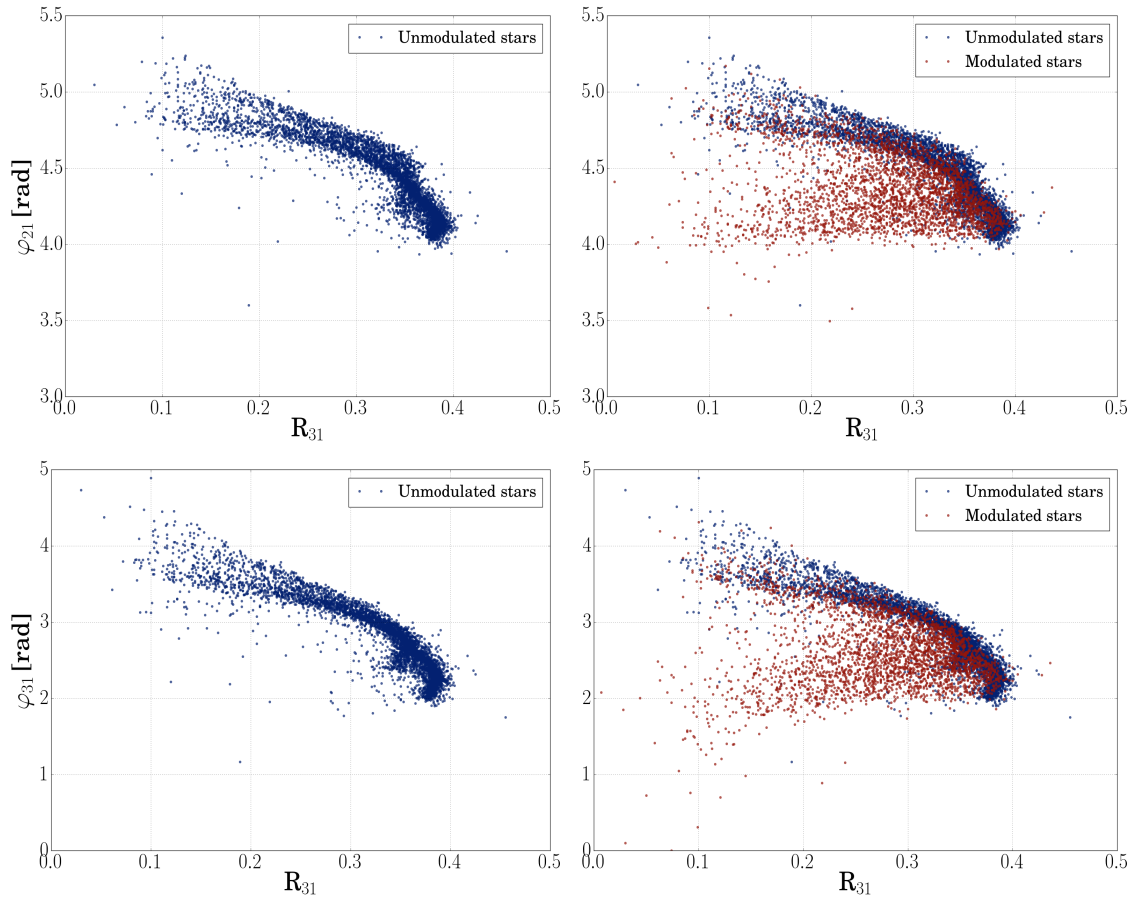


Figure 5.13: The dependence R_{31} vs. φ_{21} and R_{31} vs. φ_{31} for modulated and unmodulated stars. The left-hand figures show R_{31} – φ_{21} and R_{31} – φ_{31} dependences only for unmodulated stars, while the plots on the right-hand include modulated and unmodulated stars.

Looking at Fig. 5.13 we decided to determine relations that would give us a tool for identification of modulated stars. We used only stars that belong to the OoI (see Sect. 6.1 separation of the Oosterhoff populations). We used LLSM and iteratively removed outliers that deviated more than 3σ , and derived these equations

$$\varphi_{21} = 5.2944 - 7.5817R_{31} + 38.3686R_{31}^2 - 68.6348R_{31}^3 \quad \sigma = 0.0618, \quad (5.3)$$

$$R_{31} = 0.4410 - 0.2098\varphi_{31} + 0.1561\varphi_{31}^2 - 0.0331\varphi_{31}^3 \quad \sigma = 0.0096. \quad (5.4)$$

Results of these models are in Fig. 5.14. The fit for given equation is shown with green line, while the blue stripe represents area deviating less than 3σ .

Considering, that stars with the Blazhko effect cluster below the hook shape trend, these models can serve as identifiers of possible Blazhko stars. We decided to calculate the fraction of modulated stars located under this model. In dependence φ_{21} vs. R_{31} further than 3σ below model the population of RR Lyrae stars consists of 90 % of modulated stars. The results with an increasing integer multiplier of σ are in table 5.5.

Table 5.5: A table for the fraction of modulated stars that fell below the predicted dependences 5.3 and 5.4, based on $n\sigma$, where n is an integer. The total number of RR Lyraes in each cut is also included.

R_{31} vs. φ_{21}			φ_{31} vs. R_{31}	
$n\sigma$	% Blazhko stars	# number of stars	% Blazhko stars	# number of stars
1σ	72.5 %	3190	71.6 %	3680
2σ	81.0 %	2416	79.8 %	2981
3σ	90.5 %	1830	85.3 %	2490
4σ	94.8 %	1504	89.2 %	2125
5σ	96.6 %	1226	91.1 %	1869
\vdots	\vdots	\vdots	\vdots	\vdots
10σ	99.2 %	250	95.0 %	1020

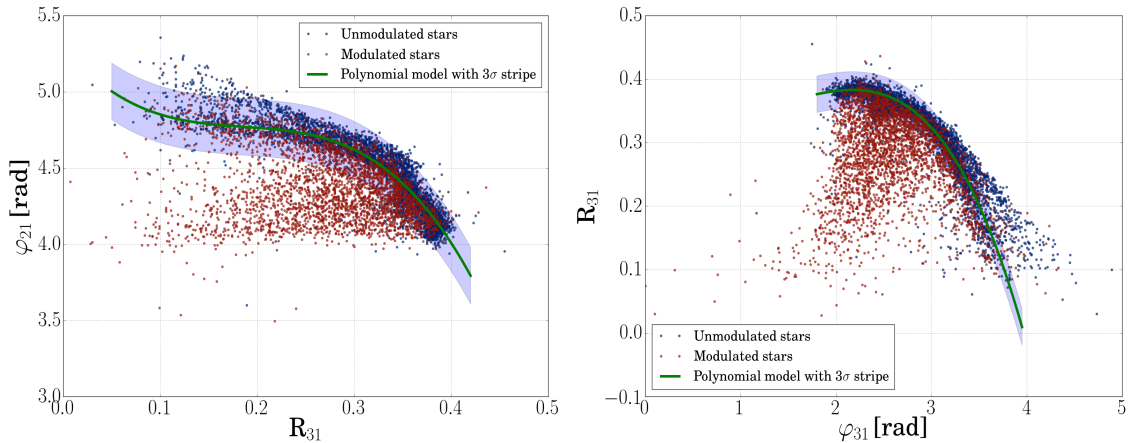


Figure 5.14: The dependence between $R_{31}-\varphi_{21}$ and $\varphi_{31}-R_{31}$ for modulated and stable stars. The left-hand panel shows $R_{31}-\varphi_{21}$ dependence for modulated (red dots) unmodulated (blue dots) stars. The green coloured fit outline the OoI population, with blue transparent stripe representing 3σ standard deviation. The right-hand panel displays $\varphi_{31}-R_{31}$ dependence with the same colour distribution of modulated and unmodulated stars as in the left-hand plot. The green coloured fit again outline the OoI population, and blue transparent stripe represents 3σ standard deviation.

For the first time in history of studying RR Lyrae stars, we see a clear difference between modulated and unmodulated stars, and we can quantitatively estimate, if a star exhibits the Blazhko effect, or not. These relations could be used in a study of the Galactic structure and in automatic procedures to identify the Blazhko stars.

We note that for the φ_{31} – R_{31} dependence, we switched the axis in comparison with the Fig. 5.13. This was due to a polynomial fit, that for this dependence, better described the hook-shape structure and separated modulated and unmodulated stars. In addition, we did not use dependences on R_{21} because modulated stars are less detached from unmodulated stars than in R_{31} plots (see Fig. 5.15). Blazhko stars in the R_{21} – φ_{31} and R_{21} – φ_{21} dependences, seem to cluster more closely to the unmodulated OoI stream. Therefore, the separation between both groups is less clear, than for R_{31} – φ_{21} and R_{31} – φ_{31} dependencies.

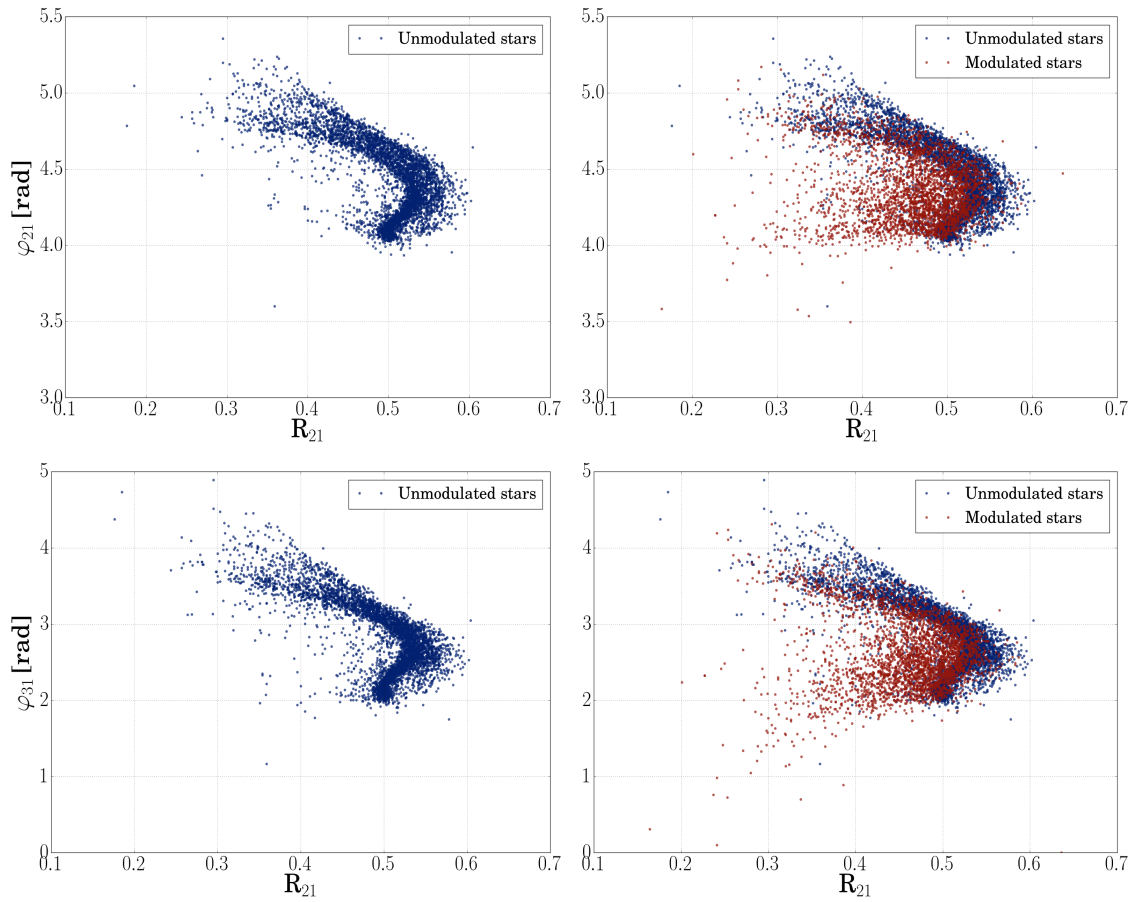


Figure 5.15: All four plots show dependence R_{21} vs. φ_{21} and R_{21} vs. φ_{31} for modulated and unmodulated stars. The left-hand figures show R_{21} – φ_{21} and R_{21} – φ_{31} dependences only for unmodulated stars, while the plots on the right-hand includes modulated and unmodulated stars.

Chapter 6

By-product results

IN the following two sections, we sum up the two important results which have emerged from the analysis. These results are not directly connected to the Blazhko effect, but they are so important, that we decided to mention them. The first is the identification of two Oosterhoff populations in the Galactic bulge. This outcome would probably remain hidden if we did not identify modulated stars. The second additional result is the discovery of so far undocumented double-mode pulsators among RRab stars. Both of these results will be further elaborated in our further studies.

6.1 Oosterhoffs populations within the Galactic bulge

Looking at the Fig. 5.13, we can safely say that there are two Oosterhoff populations in the Galactic bulge. The OoII is not very distinct in period-amplitude diagram 5.6, but stands out in figures for Fourier parameters. To determine which Oosterhoff group a star belongs to, we tried to use the relation for the OoI, proposed by Zorotovic et al. (2010). Unfortunately, this relation had been calibrated to globular clusters. Therefore, when applied to RR Lyrae stars in the Galactic bulge, the model of Zorotovic et al. (2010) was shifted to longer periods. Therefore, we decided to estimate our own relation for the mean locus of the OoI in the Galactic bulge. We used only unmodulated stars, iteratively interpolated mean locus of the OoI and subsequently removed points deviating more than 3σ . In the end of fitting process we derived polynomial relation

$$A_{I-\text{locus}}^{\text{ab}} = -1.732 - 13.544 \log P - 17.798 \log^2 P \quad , \quad \sigma = 0.034 \quad . \quad (6.1)$$

To outline the OoII we used the same procedure as Zorotovic et al. (2010). We applied the same relation as for the OoI eq. 6.1, but with a positive shift of 0.06 in $\Delta \log P$. The result of using created model on unmodulated stars is in Fig. 6.1. The solid red line displays the OoI stream and the dashed line corresponds to the presumed position of the OoII.

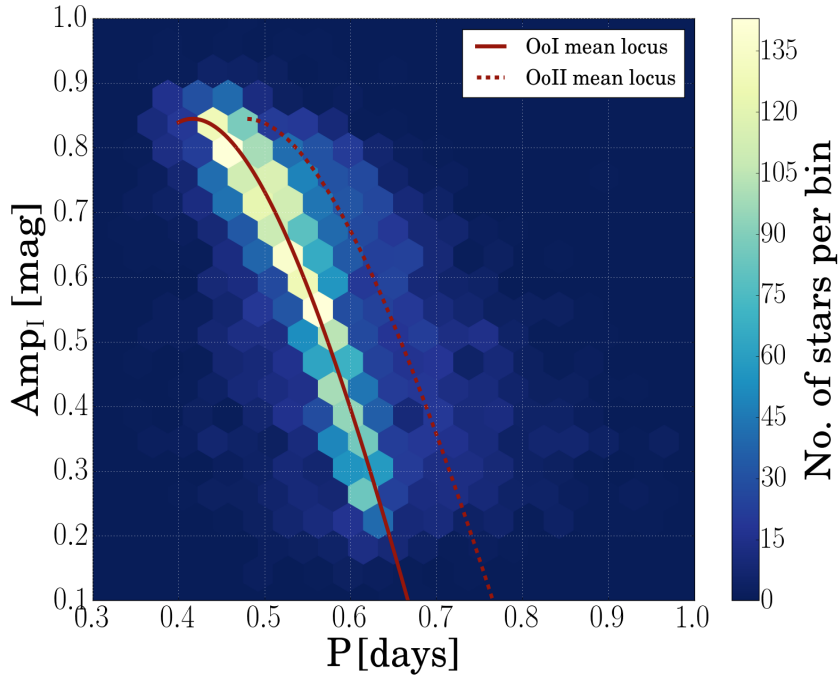


Figure 6.1: The period-amplitude density diagram for unmodulated stars, with model functions (red lines) separating the Oosterhoff populations.

Using our fit we can separate both populations and study the Blazhko effect based on the affiliation to the Oosterhoff groups. To decide whether a star belongs to the OoI or the OoII, we adopted threshold from [Miceli et al. \(2008\)](#) as $\Delta P = 0.045$ days to separate the OoI from the OoII, using this relation

$$\Delta P = P_{\text{ab}} - P_{\text{OoI-locus}} . \quad (6.2)$$

In this relation P_{ab} is the pulsation period for RRab stars from our sample and $P_{\text{OoI-locus}}$ is period calculated using eq. 6.1 for given amplitude. If a star had $\Delta P \leq 0.045$ days we included it into the OoI, if not we assigned it to OoII. When we divided all stars into the Oosterhoff groups, we investigated the distribution of the Blazhko effect. The percentage of modulated stars for the OoI is 46 %, while for the OoII it is only 19 %. For comparison with three globular clusters see table 3.1. The reasons for this discrepancy could be several. In Sect. 5.2 we showed that the incidence rate of the Blazhko effect rises for shorter periods, also, the preference of a lower amplitude might be involved as well.

The Oosterhoff groups differ not only in periods, but also in metallicity. In Fig. 6.2 on the left-hand panel, we see a distribution of metallicity between both groups. The average metallicities for unmodulated stars in the Oosterhoff groups are $[\text{Fe}/\text{H}]_{\text{OoI}} = -0.89(24)$ dex and $[\text{Fe}/\text{H}]_{\text{OoII}} = -1.27(26)$ dex. In addition, average pulsation periods for both groups are $P_{\text{OoI}} = 0.54(6)$ days and $P_{\text{OoII}} = 0.66(9)$ days. This information, together with the data from [Catelan \(2009\)](#), allowed us to construct the diagram on the right-hand panel of the Fig. 6.2. Blue dots in this plot stand for the Galactic globular clusters, green

triangles represent globular clusters from the LMC, and red stars outline two Oosterhoff populations in the Galactic bulge. We see that both populations from the Galactic bulge lie on the metal-rich side of their groups.

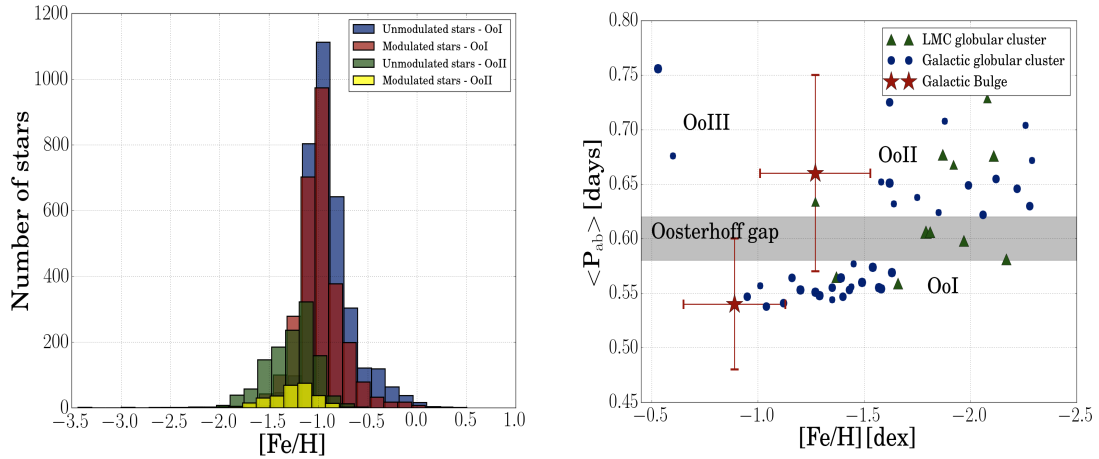


Figure 6.2: The distribution of metallicities in both Oosterhoff groups, and $[\text{Fe}/\text{H}] - \langle P_{\text{ab}} \rangle$ dependence two Oosterhoff populations in the Galactic bulge. The left-hand figure shows distribution of metallicity for the Oosterhoff populations and stars with the Blazhko effect. The right-hand image displays period-metallicity dependence for globular clusters from the LMC (green triangles) and our Galaxy (blue dots) together with two Oosterhoff groups from the Galactic bulge with error bars. Sizes of dots and triangles are based on the number of RR Lyrae stars within the globular clusters. The data for globular clusters were obtained from [Catelan \(2009\)](#).

We note that the assumed threshold from [Miceli et al. \(2008\)](#) was previously used and calibrated on globular clusters, thus it might not work perfectly on the Galactic bulge. This offers a huge opportunity to study differences between both Oosterhoff populations, with respect to the Fourier coefficients and physical parameters of both groups. A detailed analysis of both Oosterhoff groups, is, however, out of scope of this thesis, and will be the goal of our further investigation.

6.2 A new group of double-mode RR Lyrae pulsators

During the inspection of stars that were preliminarily selected as the most promising, regarding the Blazhko modulation, we identified a possible new group of double mode RR Lyrae pulsators. Among most of these stars we were not able to find side peaks in the range for the Blazhko effect, even though they exhibited changes in amplitude and phases. Thus, we performed a manual period analysis and found an additional mode in the frequency spectrum. We claim, that to confirm a multi-periodicity we need to detect combination

frequencies of the parental frequencies, in the Fourier spectrum. If a star displays multiple periods, but no combination between them, then it is probably a blend. The Fig. 6.3 shows the frequency spectrum of the discovered double-mode star. The main pulsation frequency and its harmonics were removed and are outlined by dashed lines. For clarity, we also removed daily aliases. The additional mode remained in the spectrum and is marked as $f_{0.7}$.

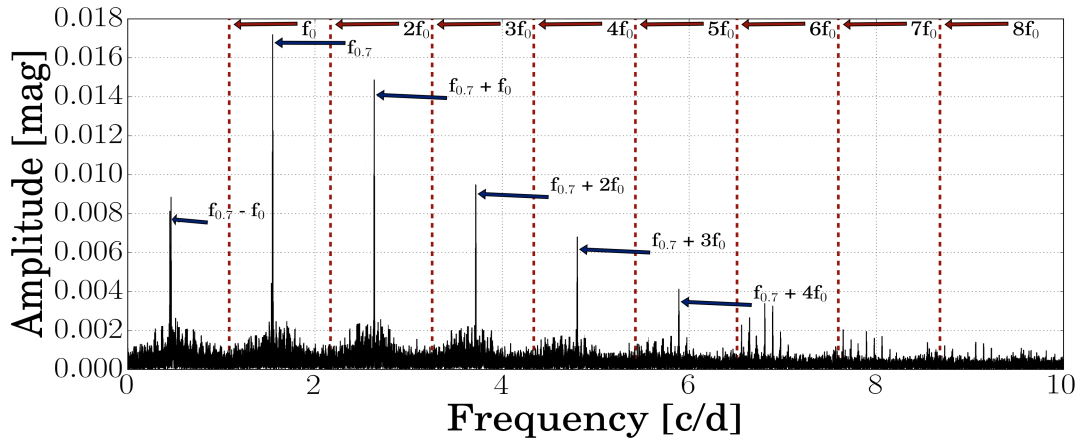


Figure 6.3: The frequency spectrum of OGLE-BLG-RRLYR-07283 with removed main pulsation frequency and its harmonic (outlined by dashed red lines). The additional mode noted as $f_{0.7}$ with its several harmonics is highlighted with blue colour. Daily aliases of the additional mode were removed to preserve clarity.

We found more than 40 RRab stars manifesting this additional mode. In Fig. 6.4 we show the Petersen diagram to compare our discovered stars with previously known double-mode variables. In this plot, we can divide our sample into four categories.

The first category consists of two stars, lying above the stream of RRd stars with the period ratio around 0.75. These stars are probably High-Amplitude δ Scuti variables, therefore they are most likely misinterpreted as RR Lyraes. In the second category, there is only one star, lying below the stream of RRd stars with the period ratio 0.727. This star was most likely misclassified as RRab, and should be reclassified as a RRd star. This star also exhibits the Blazhko effect, which makes it one of the few RRd stars with modulation.

Two stars with $\log P_{\text{LONG}} > -0.2$ days form the third group. These objects are RRab type stars and do not resemble RRd type stars, they exhibit additional mode with a strange period ratio around 0.7. This new periodicity has not been explained by hydrodynamical pulsation models so far. The preliminary results suggest that these stars have very high, almost solar-like metallicity. The third group will be thoroughly studied in Smolec et al. (2016, in prep.).

The last and the most populated group consists of RRab stars with very short periods and the period ratio around 0.7. Similarly to the third group, there has been no theoretical explanation for this second mode so far. It is important to say that the objects from the third and fourth groups do not belong

to any other category of pulsating stars. They form a new groups of RR Lyrae pulsators. In addition, the period ratio does not correspond to any of the radial mode. Stars that pulsate in the first-overtone and the fundamental mode have period ratios around 0.74 days, while stars with the second-overtone and the fundamental mode have the period ratio approximately of 0.58 days. Therefore, stars with the period ratio 0.7 do not fit into either of these categories.

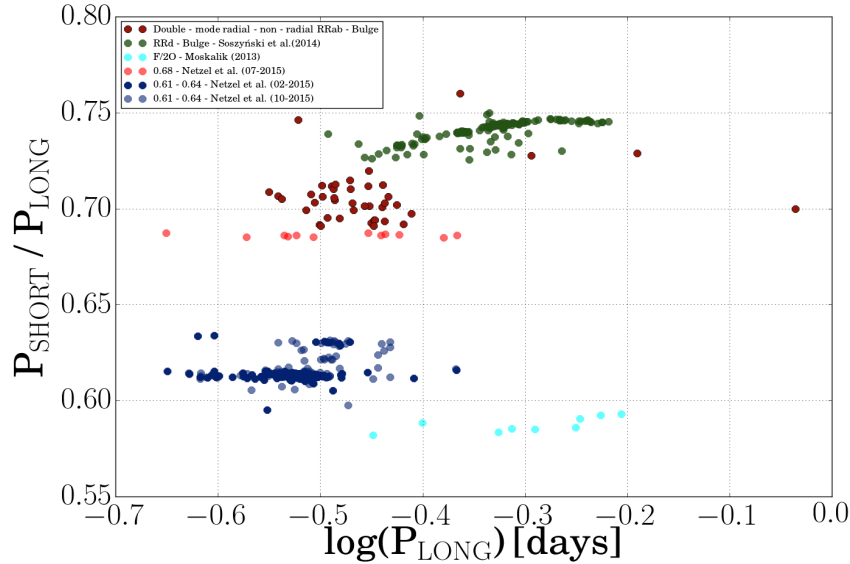


Figure 6.4: The Petersen diagram for RR Lyrae stars with an additional mode. Dark red points belong to a newly discovered RRab type stars with an extra mode. The cyan points belong to RRab stars with the Blazhko modulation that exhibits the additional second-overtone mode. The blue and light red points belong to RRc stars found by Netzel et al. (2015a,b,c). The dark green points outline RRd stars.

Not all of these stars with additional mode were included in the sample for search of the Blazhko modulation. After the discovery of the first star with 0.7 period ratio, we created an automatic procedure to analyse all RRab stars in OGLE-IV survey. The procedure consisted of NLLS method with trigonometric polynomial and implementation of the Lomb-Scargle algorithm (Herzberg & Glogowski, 2014). This program searched for significant peaks in the frequency spectrum between the main pulsation frequency and its first harmonic. Stars with a strange peak in this region were marked as candidates and analysed manually to confirm, or deny additional periodicity. Using this script we were able to find more stars with an extra mode. Several of these double-mode stars will be targeted by *Kepler* space telescope in K2 campaigns 9 & 11. Therefore, additional data can help to unravel this mystery. Thorough analysis of these stars will be targeted in our future study.

Chapter 7

Summary

THIS thesis has two main objectives – to determine the percentage of the Blazhko stars in the Galactic bulge, and investigate the relation between the pulsation and modulation periods. It is divided into seven chapters. The first three chapters are focused on the latest knowledge regarding RR Lyrae stars, methods of analysis of RR Lyrae stars and the Blazhko effect. The following chapter describes the used data from the OGLE survey and the selection of stars. In the two last chapters we discuss our results in comparison with previous studies.

We present one of the most extensive and the most homogeneous analysis of the Blazhko effect among RR Lyrae stars. We semi-automatically analysed over 8 000 RR Lyrae stars from the Galactic bulge using OGLE-IV and OGLE-III data. We found that 38 % of total sample of 8 283 stars manifest the Blazhko effect. For comparison, [Mizerski \(2003\)](#), [Collinge et al. \(2006\)](#) and [Soszyński et al. \(2011\)](#) worked with similar data but found a smaller percentage of modulated stars (25 %, 28 %, and 30 % respectively). We compared our results with the only available list of Blazhko stars in the Galactic bulge ([Collinge et al., 2006](#)). From our Blazhko sample 418 were also included in their list, we differ in twelve stars. Six stars were in our analysis marked as unmodulated and other six as possible candidates.

We look for the possible relation between modulation and pulsation periods, but we did not find any connection in our sample. The periods of the Blazhko modulation of the sample stars span from less than 5 days up to more than 2 100 days. We report a discovery of a star with the shortest Blazhko modulation, the first one with Blazhko period below 5 days. Spatial distribution of RR Lyraes do not show any overdensities of modulated, or unmodulated stars suggesting that the position has no impact to the percentage of modulated stars.

The mean of pulsation periods for Blazhko stars (0.53(6) days) differs from the average of pulsation periods of unmodulated stars (0.56(9) days). Therefore they differ by a factor 0.03 days. We note that both groups are within the error identical, but, since the distribution is highly non-Gaussian, the uncertainties could be misleading.

In addition, we found an analogous difference in amplitudes of RR Lyrae stars. It seems that stars with the Blazhko modulation have amplitudes lower of 0.028(45) mag than unmodulated stars. The difference in amplitudes was previously proposed by Szeidl (1988), thus we give his assumption particular value.

We used Fourier coefficients provided by OGLE-IV for individual stars and examined the differences between stars without modulation and stars with the Blazhko effect. We found that for parameters R_{21} and R_{31} , the ratio of the Blazhko stars differs for different values. For lower values of these coefficients the incidence rate of stars with modulation rises, and sometimes exceeds 50%. This excess is expected because we found the difference in amplitudes, and R_{21} together with R_{31} are directly connected with amplitudes. Phase parameters φ_{21} and φ_{31} likewise show differences for modulated and unmodulated stars. For φ_{31} is the difference 0.22 rad and for φ_{21} it is 0.09 rad. The occurrence of the Blazhko effect seems to decrease for larger values of these coefficients.

We exploited the separation between modulated and unmodulated stars and separated both groups using polynomial model. Then, we discuss the number of Blazhko stars that fell under the model based on integer multipliers of σ . The two presented polynomial relations, eq. 5.3 and 5.4, can help distinguish stars of the both groups. In eq. 5.3, below 3σ from the model, the percentage of modulated stars exceed 90%. The non-uniformity of ratio of the Blazhko stars in the pulsation periods and φ_{31} suggest also a difference in metallicity. However, our analysis showed that there is no global metallicity difference between modulated and unmodulated RR Lyrae stars at all.

While studying Fourier coefficients for RR Lyrae in the Galactic bulge, we noticed two Oosterhoff populations. We divided both groups, using procedures described in Zorotovic et al. (2010) and Miceli et al. (2008). Subsequently we were able to study the distribution of Blazhko stars in each Oosterhoff group. The OoI has 46% of modulated stars while the OoII has only 19% of Blazhko stars. We managed to calculate average metallicity for each group ($[\text{Fe}/\text{H}]_{\text{OoI}} = -0.89(24)$ dex and $[\text{Fe}/\text{H}]_{\text{OoII}} = -1.27(26)$ dex). Both groups have higher metallicities in comparison with other stellar systems in respective Oosterhoff populations.

In addition to analysis of the Blazhko effect, we discovered a new subclass of double-mode RR Lyrae pulsators. These stars cluster around period ration of 0.7 and form two groups in the Petersen diagram. So far, no RR Lyraes had been reported with a similar period ratio, and there is no theoretical background to explain such behaviour.

Despite interesting new discoveries, new questions arose. This seems to be typical for studying the Blazhko effect. The results from this thesis offer an opportunity for many future studies. Hopefully, this thesis will contribute to better understanding the long-lasting Blazhko mystery.

Bibliography

- Alard, C., & Lupton, R. H. 1998, *ApJ*, 503, 325
- Alard, C. 2000, *A&AS*, 144, 363
- Alcock, C., Alves, D. R., Becker, A., et al. 2003, *ApJ*, 598, 597
- Bailey, S. I. 1902, *Annals of Harvard College Observatory*, 38, 1
- Benkő, J. M., Kolenberg, K., Szabó, R., et al. 2010, *MNRAS*, 409, 1585
- Benkő, J. M., Szabó, R., & Paparó, M. 2011, *MNRAS*, 417, 974
- Benkő, J. M., Plachy, E., Szabó, R., et al. 2014, *ApJS*, 213, 31
- Blažko, S. 1907, *Astronomische Nachrichten*, 175, 327
- Bryant, P. H. 2014, *ApJL*, 783, L15
- Buchler, J. R., & Kolláth, Z. 2011, *ApJ*, 731, 24
- Carroll W. B, Ostlie D. A., 2007, *An introduction to modern astrophysics*, Pearson Education Inc., San Francisco
- Catelan, M. 2009, *Ap&SS*, 320, 261
- Catelan, M., & Smith, H. A. 2015, *Pulsating Stars* (Wiley-VCH)
- Collinge, M. J., Sumi, T., & Fabrycky, D. 2006, *ApJ*, 651, 197
- Cox, J. P. 1958, *ApJ*, 127, 194
- Dorfi, E. A., & Feuchtinger, M. U. 1999, *A&A*, 348, 815
- Dziembowski, W. A. 2015, in press, preprint arXiv:1512.03708
- Eddington, A. S., 1918, *MNRAS*, 79, 2
- Eddington, A., 1926, *The Internal Constitution of the Stars*, Cambridge: Cambridge University Press, 1926. ISBN 9780521337083
- Arellano Ferro, A., Bramich, D. M., Figuera Jaimes, R., et al. 2012, *MNRAS*, 420, 1333

- Gillet, D. 2013, *A&A*, 554, A46
- Gillet, D., Fabas, N., & Lèbre, A. 2013, *A&A*, 553, A59
- Gruberbauer, M., Kolenberg, K., Rowe, J. F., et al. 2007, *MNRAS*, 379, 1498
- Guggenberger, E., Kolenberg, K., Nemeč, J. M., et al. 2012, *MNRAS*, 424, 649
- Hajdu, G., Catelan, M., Jurcsik, J., et al. 2015, *MNRAS*, 449, L113
- Herzberg, W., & Glogowski, K. 2014, *Precision Asteroseismology*, 301, 421
- Jurcsik, J., & Kovacs, G. 1996, *A&A*, 312, 111
- Jurcsik, J. 1998, *A&A*, 333, 571
- Jurcsik, J., Szeidl, B., Nagy, A., et al. 2005, *AcA*, 55, 303
- Jurcsik, J., Sódor, Á., Szeidl, B., et al. 2009, *MNRAS*, 400, 1006
- Jurcsik, J., Szeidl, B., Clement, et al. 2011, *MNRAS*, 411, 1763
- Jurcsik, J., Hajdu, G., Szeidl, B., et al. 2012, *MNRAS*, 419, 2173
- Jurcsik, J., Smitola, P., Hajdu, G., & Nuspl, J. 2014, *ApJL*, 797, L3
- Jurcsik, J., Smitola, P. 2016, in preparation
- Kinemuchi, K., Smith, H. A., Woźniak, et al. 2006, *AJ*, 132, 1202
- Kolláth, Z., Molnár, L., & Szabó, R. 2011, *MNRAS*, 414, 1111
- Le Borgne, J. F., Poretti, E., Klotz, A., et al. 2014, *MNRAS*, 441, 1435
- Lenz, P., & Breger, M. 2004, *The A-Star Puzzle*, 224, 786
- Levenberg, K., 1944, *Quarterly of Applied Mathematics* 2: 164–168
- Liška, J. 2015, *Changes of orbital periods in binary systems*, Masaryk University, Brno, [Dissertation]
- Marquardt, D., 1963, *SIAM Journal on Applied Mathematics* 11 (2): 431–441
- Miceli, A., Rest, A., Stubbs, C. W., et al. 2008, *ApJ*, 678, 865
- Mikulášek, Z., & Zejda M., 2013, *Úvod do studia proměnných hvězd*, Masaryk University, Brno, [textbook]
- Mizerski, T. 2003, *AcA*, 53, 307
- Moskalik, P., & Poretti, E. 2003, *A&A*, 398, 213
- Moskalik, P., & Kołaczkowski, Z. 2009, *MNRAS*, 394, 1649

- Moskalik, P. 2013, *Stellar Pulsations: Impact of New Instrumentation and New Insights*, 31, 103
- Moskalik, P., Smolec, R., Kolenberg, K., et al. 2015, *MNRAS*, 447, 2348
- Nemec, J. M. 1985, *AJ*, 90, 240
- Netzel, H., Smolec, R., & Moskalik, P. 2015a, *MNRAS*, 447, 1173
- Netzel, H., Smolec, R., & Dziembowski, W. 2015b, *MNRAS*, 451, L25
- Netzel, H., Smolec, R., & Moskalik, P. 2015c, *MNRAS*, 453, 2022
- Oosterhoff, P. T. 1939, *The Observatory*, 62, 104
- Petersen, J. O. 1973, *A&A*, 27, 89
- Pickering, E. C. 1901, *Astronomische Nachrichten*, 154, 423
- Pietrukowicz, P., Kozłowski, S., Skowron, J., et al. 2015, *ApJ*, 811, 113
- Poretti, E., Le Borgne, J.-F., Klotz, et al. 2016, arXiv:1601.02772
- Sandage, A. 1958, *Ricerche Astronomiche*, 5, 41
- Schwarzschild, M. 1940, *Harvard College Observatory Circular*, 437, 1
- Shapley, H. 1914, *ApJ*, 40, 448
- Shapley, H. 1916, *ApJ*, 43, 217
- Shibahashi, H. 2000, *IAU Colloq. 176: The Impact of Large-Scale Surveys on Pulsating Star Research*, 203, 299
- Simon, N. R., & Lee, A. S. 1981, *ApJ*, 248, 291
- Simon, N. R. 1988, *ApJ*, 328, 747
- Skarka, M. 2013, *A&A*, 549, A101
- Skarka, M., & Zejda, M. 2013, *MNRAS*, 428, 1442
- Skarka, M. 2014, *A&A*, 562, A90
- Skarka, M. 2014, *MNRAS*, 445, 1584
- Skarka, M., Liška, J., Auer, R. F., Prudil, Z., Juráňová, A., Sódor, Á., 2016, submitted to *A&A*
- Smith A. Horace, 1995, *RR Lyrae stars*, Cambridge university press, Cambridge
- Smolec, R. 2005, *AcA*, 55, 59

- Smolec, R., & Moskalik, P. 2012, *MNRAS*, 426, 108
- Smolec, R., Soszyński, I., Udalski, A., et al. 2015, *MNRAS*, 447, 3756
- Smolec, R. 2016, in press, preprint arXiv:1603.01252
- Smolec, R., Prudil, Z., Skarka, M., Bąkowska, K., 2016, in preparation
- Soszyński, I., Udalski, A., Szymański, M. K., et al. 2009, *AcA*, 59, 1
- Soszyński, I., Udalski, A., Szymański, M. K., et al. 2010, *AcA*, 60, 165
- Soszyński, I., Dziembowski, W. A., Udalski, A., et al. 2011, *AcA*, 61, 1
- Soszyński, I., Udalski, A., Szymański, M. K., et al. 2014, *AcA*, 64, 177
- Stellingwerf, R. F., Gautschi, A., & Dickens, R. J. 1987, *ApJL*, 313, L75
- Szabó, R., Kolláth, Z., Molnár, L., et al. 2010, *MNRAS*, 409, 1244
- Szczygieł, D. M., & Fabrycky, D. C. 2007, *MNRAS*, 377, 1263
- Szeidl, B. 1976, *IAU Colloq. 29: Multiple Periodic Variable Stars*, 60, 133
- Szeidl, B. 1988, *Multimode Stellar Pulsations*, 45
- Szeidl, B., Hurta, Z., Jurcsik, J., Clement, C., & Lovas, M. 2011, *MNRAS*, 411, 1744
- Udalski, A., Szymanski, M., Kaluzny, J., Kubiak, M., & Mateo, M. 1992, *AcA*, 42, 253
- Udalski, A., Szymański, M. K., & Szymański, G. 2015, *AcA*, 65, 1
- Van Hoolst, T., Dziembowski, W. A., & Kawaler, S. D. 1998, *A Half Century of Stellar Pulsation Interpretation*, 135, 232
- Vandenbroere, J., Poretti, E., & Le Borgne, J.-F. 2012, in press, preprint arXiv:1202.3546
- Viaux, N., Catelan, M., Stetson, P. B., et al. 2013, *A&A*, 558, A12
- Watson, C. L. 2006, *Society for Astronomical Sciences Annual Symposium*, 25, 47
- Wozniak, P. R. 2000, *AcA*, 50, 421
- Zhevakin, S. A. 1953, *Russ A.J.*, 30, 161
- Zorotovic, M., Catelan, M., Smith, H. A., et al. 2010, *AJ*, 139, 357

